ABSTRACT

Title of dissertation: DESIGN AND IMPLEMENTATION OF INFORMATION PATHS IN DENSE WIRELESS SENSOR NETWORKS

Masoumeh Haghpanahi,
Doctor of Philosophy, 2011

Dissertation directed by: Professor Mark Shayman
Department of Electrical and Computer Engineering

In large-scale sensor networks with monitoring applications, sensor nodes are responsible to send periodic reports to the destination which is located far away from the area to be monitored. We model this area (referred to as the distributed source) with a positive load density function which determines the total rate of traffic generated inside any closed contour within the area.

With tight limitations in energy consumption of wireless sensors and the many-to-one nature of communications in wireless sensor networks, the traditional definition of connectivity in graph theory does not seem to be sufficient to satisfy the requirements of sensor networks. In this work, a new notion of connectivity (called implementability) is defined which represents the ability of sensor nodes to relay traffic along a given direction field, referred to as information flow vector field $\vec{D}$. The magnitude of information flow is proportional to the traffic flux (per unit length) passing through any point in the network, and its direction is toward the flow of traffic. The flow field may be obtained from engineering knowledge or as a solution

to an optimization problem. In either case, information flow flux lines represent a set of abstract paths (not constrained by the actual location of sensor nodes) which can be used for data transmission to the destination. In this work, we present conditions to be placed on $\vec{D}$ such that the resulting optimal vector field generates a desirable set of paths.

In a sensor network with a given irrotational flow field $\vec{D}(x, y)$, we show that a density of $n(x, y) = O(|\vec{D}(x, y)|^2)$ sensor nodes is not sufficient to implement the flow field as $|\vec{D}|$ scales linearly to infinity. On the other hand, by increasing the density of wireless nodes to $n(x, y) = O(|\vec{D}(x, y)|^2 \log |\vec{D}(x, y)|)$, the flow field becomes implementable. Implementability requires more nodes than simple connectivity. However, results on connectivity are based on the implicit assumption of exhaustively searching all possible routes which contradicts the tight limitation of energy in sensor networks. We propose a joint MAC and routing protocol to forward traffic along the flow field. The proposed tier-based scheme can be further exploited to build lightweight protocol stacks which meet the specific requirements of dense sensor networks.

We also investigate buffer scalability of sensor nodes routing along flux lines of a given irrotational vector field, and show that nodes distributed according to the sufficient bound provided above can relay traffic from the source to the destination with sensor nodes having limited buffer space. This is particularly interesting for dense wireless sensor networks where nodes are assumed to have very limited resources.

DESIGN AND IMPLEMENTATION OF INFORMATION PATHS IN DENSE WIRELESS SENSOR NETWORKS

by

Masoumeh Haghpanahi

Dissertation submitted to the Faculty of the Graduate School of the
University of Maryland, College Park in partial fulfillment
of the requirements for the degree of
Doctor of Philosophy
2011

Advisory Committee:
Professor Mark A. Shayman, Chair/Advisor
Dr. Mehdi Kalantari, Co-Advisor
Professor K. J. Ray Liu
Professor Richard J. La
Professor Lawrence C. Washington

Dedication

To my sources of motivation:

my grandmother, my parents and my husband

Acknowledgments

It is a pleasure to thank those who made this thesis possible. First and foremost, I would like to express my sincere gratitude to my advisor, Professor Mark Shayman for his guidance and support throughout the course of my graduate studies. Our group meetings and discussions have been invaluably educational; his attention to mathematical rigor and concise thinking have significantly improved my technical communication skills.

I would like to thank Professors K. J. Ray Liu, Richard J. La, Lawrence C. Washington and Dr Mehdi Kalantari for agreeing to serve on my thesis committee. Special thanks to Dr Mehdi Kalantari for his great enthusiasm and forward-thinking vision in our mutual discussions and group meetings which led to fruitful research.

I am grateful to all the administrative staff of the ISR and ECE department, and all my friends who have helped me in various ways. I will not forget all the good times we had together and all the support that I have received from them.

I would like to specially thank Professor Andre L. Tits, for I have learnt and benefited a lot from his lectures, constructive conversations, mentorship, and friendship.

Finally, I would like to thank my parents for their endless support and love, and my beloved husband, Masoud, for his support and patience throughout this journey. Without them, I would not have been able to accomplish this achievement.

Table of Contents

List of Figures

List of Abbreviations

a.s.	almost surely
BPI	Bounded Physical Interference
bps	bits per second
CH	Cluster Head
FCFS	First-Come-First-Served
GUI	Graphical User Interface
i.i.d	independent and identically distributed
LOS	Line of Sight
ODE	Ordinary Differential Equation
pps	packets per second
SINR	Signal to Interference Plus Noise Ratio
SLLN	Strong Law of Large Numbers
w.h.p	with high probability
WSN	Wireless Sensor Networks

Chapter 1

Introduction

1.1 Motivation

With recent advances in hardware technology, low-cost processors, miniature sensing and radio modules required for sensor networks have been made, and further improvements in cost and capabilities are expected within the next decade [60–62].

A Wireless Sensor Network (WSN) is composed of a large number of sensor nodes densely deployed inside or very close to a phenomenon. The exact position of sensors need not be predetermined, and they can be randomly deployed in inaccessible terrains. Such networks are usually aimed at monitoring vast regions, much larger than the transmission radius of an individual node. Therefore, data transmission occurs in multihop communication. There has arisen a great demand for sensor networks in many fields including military, environment monitoring, transportation systems and agriculture [60, 63, 64].

WSN applications are classified based on their data-delivery requirements and their traffic characteristics. According to [5], most of the current WSN applications fall into one of the following broad classes of (i) monitoring and periodic reporting, (ii) event detection and reporting, (iii) sink-initiated reporting, (iv) object detection and tracking, and (v) hybrid applications with more than one of the above four characteristics.

Realization of sensor network applications require wireless ad hoc networking techniques. Although many protocols have been developed for wireless ad hoc networks, they do not satisfy the unique requirements and features of sensor networks. Specific characteristics of WSNs distinguish these networks from ad hoc networks. Unlike in an ad hoc network, where any node can potentially communicate with any other node, a WSN exhibits the many-to-one communication paradigm. Also, sensor nodes have very limited energy, processing, and storage capacities. Thus, they require careful resource management. Moreover, design requirements of a sensor network change with its application. For example, while low latency is of utmost importance in applications such as tactical surveillance, extending network lifetime is more important for applications such as periodic weather monitoring [11].

It is desirable to present a framework to study WSNs that can support more than one application and to provide a means to calculate required density of sensor nodes that satisfy the throughput requirement of the network under different scenarios. To this end, we use a continuous space model called information flow vector field to model flow of traffic in WSNs. The flow field has two components (magnitude and direction) at each point in the Euclidean space; the magnitude of information flow is proportional to the traffic flux (per unit length) passing through any point in the network, and its direction is toward the flow of traffic. This is very similar to visualization of fluid flows or electric fields by means of vector fields. In fluid flow visualization for example, the flow vector field represents the fluid velocity field and flow streamlines are trajectories of massless particles that are traversed by fluid particles in the flow field as a function of time. Similarly, information flow flux

lines are a set of abstract paths used for data transmission to the destination. Note that flow flux lines are not constrained by the location of sensor nodes. This model was first introduced in [1] and [2] with an inspiration from electrostatics.

In a particular application, the flow field may be obtained from engineering knowledge. Alternatively, it may be obtained as a solution to an optimization problem.

Our focus in this work is on monitoring applications where sensor nodes deployed inside a *distributed source* send periodic reports to the destination, which is located far away from the sensor nodes. For such networks, we present a general method for flow optimization by minimizing the *p-norm* of the information flow vector field subject to basic flow constraints. We further show through numerical analysis that the *p-norm* problem has load balancing property, and that the amount of load balancing increases by increasing the value of parameter p from 1 to infinity. Specifically, when p is close to 1, optimal paths tend to pass through geometric shortest paths from the source to the destination. By increasing the value of p from 1, the optimization tries to spread the traffic in the network, and as $p \to \infty$ the results achieve maximum load balancing. Traffic forwarded along flow flux lines of the solution of the *p-norm* problem will observe different amount of load balancing based on the value of p. In practice, p can be selected based on a trade-off between delay and balancing the traffic over the network.

Next, we concentrate on the study of required density of sensor nodes inside the distributed source so that the whole area is covered and that the active set of nodes constitute a connected set such that all the traffic generated inside the source

can be forwarded to the boundary of this region.

We also study the required density of sensor nodes between the distributed source and destination to forward traffic along an irrotational information flow vector field. We show that following the optimal paths for flow of traffic requires more nodes than providing network connectivity. To perform this analysis, a new notion of connectivity called implementability is defined which represents the ability of sensor nodes to forward traffic along flux lines of a given direction field as the amount of traffic scales linearly to infinity. The implementability analysis is accompanied by proposing a controlled access scheduling scheme with which nodes can forward traffic along the flow flux lines of an irrotational flow field.

Finally, we show that following flow flux lines of a given direction field provides a means to better study buffer scalability of sensor nodes in large-scale WSNs. In particular, we show that when nodes communicate based on the proposed scheduling scheme, such analysis can be simplified to studying a linear network. Using the results from linear networks, we show that sensor nodes can forward traffic to the destination with limited buffer spaces without degrading the performance of the network, as the magnitude of traffic scales linearly to infinity.

1.2 Notations and Definitions

In this section, we state the main notations and definitions used throughout this work. This is not a comprehensive list and more notations are introduced when required.

1.2.1 Notations

Throughout this work, X $= (x, y)$ represents the Cartesian coordinates of a point in Euclidean plane $\mathbb{R}^2$. The notation $\vec{v} = (v_x, v_y)$ is used to refer to a vector field, where v_x and v_y denote the field components along the x and y axes, respectively.

In partial differential equations, the nabla operator ∇ in two-dimensional Cartesian coordinates is defined as a vector differential operator $\nabla \equiv \frac{\partial}{\partial x}\vec{a}_x + \frac{\partial}{\partial y}\vec{a}_y$, where $\vec{a}_x$ and $\vec{a}_y$ are the unit vectors along x and y axes, respectively.

The divergence of a vector field $\vec{v}$ at a point is defined as the net outward flux of $\vec{v}$ per unit area as the area about the point tends to zero [27]. For an area with an enclosed contour there will be an excess of outward or inward flux through the contour only when the area contains a source or a sink, respectively. The net outward flux per unit area is therefore a measure of the strength of the enclosed source. Using the above definition, the divergence of a vector field $\vec{v}$ in two-dimensional Cartesian coordinates can be shown to be equal to

$$\nabla \cdot \vec{v} = \frac{\partial v_x}{\partial x} + \frac{\partial v_y}{\partial y}. \tag{1.1}$$

On the other hand, the curl of vector field $\vec{v}$ is denoted by $\nabla \times \vec{v}$; its magnitude represents the maximum net circulation of $\vec{v}$ per unit area as the area tends to zero, and its direction is perpendicular to the area [27]. In two-dimensional Cartesian

coordinates,

$$\begin{aligned} \nabla \times \vec{v} &= (-\frac{\partial v_x}{\partial y} + \frac{\partial v_y}{\partial x})\vec{a}_z, \\ \text{where, } \vec{a}_z &= \vec{a}_x \times \vec{a}_y \end{aligned} \tag{1.2}$$

In vector calculus, vector fields with zero-divergence are commonly termed as incompressible (or solenoidal) and vector fields with zero-curl are termed as irrotational.

The *p-norm* of a vector $X = (x_1, x_2, \cdots, x_n) \in \mathbb{R}^n$ is defined as

$$|X|_p = \Big(\sum_{i=1}^{n} |x_i|^p \Big)^{\frac{1}{p}}, \text{ for } p \geq 1$$

Similarly, the *p-norm* of a function $f : A \to \mathbb{R}^2$ defined over a subset A of $\mathbb{R}^2$ is defined as

$$|f|_p = \Big(\int_A |f(x,y)|^p \mathrm{d}x\mathrm{d}y \Big)^{\frac{1}{p}}$$

Another measure for calculating the norm of a function f defined over A is called the *supremum norm*[1] or *uniform norm* and is defined as

$$|f|_u = \sup\{|f(x,y)| : (x,y) \in A\}$$

This can be used to define a mode of convergence; a sequence f_n of functions converges *uniformly* to a function f on a set A provided that $\lim_{n\to\infty} |f_n - f|_u = 0$.

Throughout the work, when performing linear algebra operations, a vector is

[1]The maximum might not exist if f is not continuous on its domain of definition, so the supremum is used instead [65].

treated as a column vector and B^T refers to the transpose of matrix B.

In this work we are mainly concerned with events that occur with high probability (w.h.p); that is, with probability tending to one as the argument of the function representing the event goes to infinity. We use standard notational conventions for asymptotic analyses. Hence, for two non-negative functions $f(\cdot)$ and $g(\cdot)$, $f(n) = O(g(n))$ w.h.p, if there exists a positive constant k such that $\lim_{n\to\infty} P(f(n) \leq kg(n)) = 1$. With the above notation, $f(n) = \Omega(g(n))$, as $n \to \infty$, if $g(n) = O(f(n))$. Also, $f(n) = \Theta(g(n))$ w.h.p, if there exist positive constants k_1 and k_2 such that $\lim_{n\to\infty} P(k_1 g(n) \leq f(n) \leq k_2 g(n)) = 1$. On the other hand, $f(n) = o(g(n))$, if $\lim_{n\to\infty} \frac{f(n)}{g(n)} = 0$.

Also note that throughout this work, $\log(\cdot)$ refers to the natural logarithm (logarithm to the base e).

1.2.2 Definitions

Consider a general network with predefined sources and sinks, where N nodes are distributed uniformly at random and independent from each other throughout the network. Data is sent from node to node in a multihop fashion from a source to an intended sink. For simplicity, we assume that time is slotted. Due to spatial diversity, at each time instant more than one node can transmit data to its next hop node, without facing destructive interference from other transmissions at the same time. Two models for multihop communication called the *Protocol Model* and the *Physical Model* have been proposed and widely used in the literature [13]. In

a homogeneous scenario, where sensor nodes have same transmission radius r_t and transmission power p_t, the aforementioned communication models can be described as below.

Let X_i denote the location of a node as well as the node itself. A transmission from node X_i to node X_j is successful

1. Under the Protocol Model if:

   (a)

$$|X_i - X_j| \leq r_t, \tag{1.3}$$

   where $|\cdot|$ represents the Euclidean distance between two points in the Cartesian plane, and

   (b) for every other node X_k simultaneously transmitting over the same channel,

$$|X_k - X_j| \geq (1 + \Delta) r_t \tag{1.4}$$

   $\Delta > 0$ is a nonnegative parameter which models a guard zone around the receiving node to limit interference from other nodes. It imposes the constraint that no other neighboring nodes within the guard zone of the receiver can simultaneously send data in the same channel. Hence, the Protocol Model can be restated using circular guard zones around interfering transmitters.

Let $r_I = q_I r_t, q_I \geq 1$ denote the *interference radius* of each node transmitting data. Therefore, all nodes inside a disk of radius r_I from a transmitter node receive noticeable amount of interference. Then, a communication from node X_i to X_j is successful if $|X_i - X_j| \leq r_t$ and X_j lies in the interference zone of no other nodes transmitting at the same time as X_i.

2. Under the Physical Model if: the *Signal to Interference Plus Noise Ratio (SINR)* is above a certain threshold Γ; i.e.,

$$SINR = \frac{\frac{p_t}{|X_i - X_j|^\alpha}}{N_0 + \sum_{\substack{k \in T \\ k \neq i}} \frac{p_t}{|X_k - X_j|^\alpha}} \geq \Gamma, \tag{1.5}$$

where $\{X_k, k \in T\}$ is the set of nodes simultaneously transmitting over the same channel as X_i, and N_0 refers to the ambient noise power level. This models a situation where signal power decays with distance r as $\frac{1}{r^\alpha}$. The loss factor $\alpha > 2$ in practical situations.

While the Protocol Model describes the effects of interference based on a pairwise relation between nodes, the Physical Model takes the aggregate interference into account. Because of this, the Physical Model is generally considered to be more accurate than the Protocol Model. However, the simplicity of the Protocol Model has motivated its use in design and evaluation of communication protocols [38].

In order to reduce the complexity of studying successful transmissions under the Physical Model, approximate versions of this model have been proposed in the literature, especially for network simulators [67, 68]. A Bounded Physical Interfer-

ence model (BPI model) is defined in [28] which neglects the effects of interference from nodes residing outside a region (referred to as interference region) enclosing the receiver of a particular transmission. Interference regions are considered to be circular regions, which can be characterized by a single parameter, referred to as the interference range. Hence, in a more general scenario where sensor nodes have different transmission powers, a transmission from node X_i to node X_j is successful under the BPI model if

$$SINR = \frac{\frac{p_{t,i}}{|X_i - X_j|^\alpha}}{N_0 + \sum_{\substack{k \in T \cap IR(X_j) \\ k \neq i}} \frac{p_{t,k}}{|X_k - X_j|^\alpha}} \geq \Gamma, \tag{1.6}$$

where $IR(X_j)$ denotes the interference region of node X_j.

For a detailed discussion on modeling interference in wireless ad hoc networks see [38].

1.3 Dissertation Outline

1.3.1 Introduction to Information Flow Vector Field

In Chapter 2, we define information flow vector field, and briefly point out the constraints it must satisfy in order to model flow of traffic in a general network.

We also present a general method for flow optimization in WSNs by minimizing the *p-norm* of the information flow vector field subject to basic flow constraints, namely flow conservation constraint and boundary constraint. We refer to this problem as the *p-norm* flow optimization, and show through numerical analysis

that the *p-norm* problem has load balancing property.

1.3.2 Topology Control Inside the Distributed Source

In Chapter 3, we concentrate on the study of required density of nodes inside the distributed source. Nodes inside the distributed source monitor (sense) the region and forward the traffic generated from other sensor nodes in the region. Hence, they must provide both coverage and connectivity.

1.3.3 Topology Control Between the Distributed Source and Destination

In Chapter 4, we study the required density of nodes between the distributed source and destination to forward traffic along an irrotational direction field. To perform this analysis, a new notion of connectivity called implementability is defined which represents the ability of sensor nodes to forward traffic along flux lines (also referred to as flow streamlines) of a given direction field as the amount of traffic scales linearly to infinity. The final results indicate that for an irrotational flow field $\vec{D}(x, y)$, a density of $n(x, y) = O(|\vec{D}(x, y)|^2)$ sensor nodes is not sufficient to relay traffic along the flow streamlines. On the other hand, we show that $\vec{D}(x, y)$ is implementable with a density of $n(x, y) = O(|\vec{D}(x, y)|^2 \log |\vec{D}(x, y)|)$ sensor nodes as $|\vec{D}|$ scales linearly to infinity.

1.3.4 Scalability Property with Fading and Limited Buffer Capacity

In the first part of Chapter 5, we investigate the effects of fading on implementability of information flow field. We show that under a general model of fading presented in [7], the sufficient bound on density of nodes for implementing flow paths need not be changed.

In the second part of this chapter, we deviate from using a slotted system and replace it with an asynchronous system with random transmission times. Under the asynchronous system assumption, we investigate buffer scalability of sensor nodes forwarding traffic along flow streamlines of an irrotational direction field, and show that the performance of the network does not degrade as the network size grows to infinity while sensor nodes have limited buffer space. This result is particularly interesting for dense WSNs where nodes are assumed to have very limited resources.

Chapter 2

Introduction to Information Flow Vector Field

2.1 Overview

2.1.1 Motivation

In this chapter, we present an overview of the definition of information flow vector field as defined in [1], and briefly point out the constraints it must satisfy in order to model flow of traffic in a general network.

The information flow field represents a set of paths for transmitting traffic from the distributed source to the destination, which are not constrained by the location of sensor nodes. In WSNs with monitoring and periodic reporting applications, distributed source refers to the part of the network region from which periodic reports are generated to be sent to the destination. In a particular application, the flow field may be obtained from engineering knowledge. Alternatively, it may be obtained as a solution to an optimization problem.

As introduced in [4], the *p-norm* problem places additional conditions on the flow field such that the resulting vector field generates a desirable set of paths for flow of traffic to the destination. The *p-norm* problem has load balancing property. In practice, p must be selected based on a trade-off between delay and balancing the traffic over the network.

2.1.2 Related Work

In recent years, researchers have introduced analogies between wireless networks and various disciplines of physics. For example, it was shown in [57] that a variable traffic density in a dense wireless ad hoc network results in minimum-cost routes similar to rays of light resulting from a variable optical density. This analogy between optimal routing in wireless networks and geometrical optics was later extended in [58] and [59].

In a different line of works, it was shown that by choosing a proper cost function, the optimal distribution of traffic in a WSN has the same properties of an electrostatic field. This was first studied by Kalantari and Shayman [1, 2], and was followed by Toumpis and Tassiulas [10, 40], where the authors claimed that minimizing the quadratic cost function results in optimal deployment of sensors by minimizing total number of sensors required to transport the information to the intended sinks. The problem of flow optimization was later pursued in [3], for the case with multiple commodity flows, and in [19] for the case of multi-sink sensor networks.

Analogies to electrostatics have been used in other works as well. Authors in [29] proposed a routing protocol by use of electrostatic potentials. The proposed solution introduces a potential field that covers the network such that each node is associated with a given potential value. The packets are then routed through nodes with a decreasing potential value. This formulation has been extended to deal with anycasting and is extensively investigated in [16] in which a heat-inspired model for

link-diversity routing is presented. The heat equation in steady state follows the Laplace equation. To exploit this property for routing, the destination in a network is modeled as a heat source. Then, the heat flow resulting from the source at all the nodes is evaluated according to the network connectivity. Once all the values are calculated, finding a path from the source to the destination is a gradient search problem. This way, the path followed by a packet resembles the minimum-energy diffusion path of a particle in a temperature field.

In [15], Nguyen et al. consider establishing a framework for routing by using an analogy with electric fields. The authors proposed the use of several electric flux lines generated by placing a positive charge in the source and a negative charge in the destination as routes.

A common assumption used in many of these works is that the number of nodes is very large or that the wireless network is "dense".

2.2 Modeling Flow of Traffic in WSNs

Consider sensor networks with the application of monitoring and sending periodic reports to the destination. The destination is assumed to have unlimited energy, space and processing power, and is usually far away from the region to be monitored. Each sensor monitors a neighboring region around itself and periodic reports are sent in a multihop fashion to the destination (also referred to as the information sink). For now, we assume that sensor nodes are distributed and communicate in such a way that the correlation between data generated by neighboring

sensor nodes are removed before transmitting traffic to the destination. This will be addressed more in detail in Chapter 3.

We model the geographical area which must be monitored with a positive load density function $\rho(x, y)$. The closure of this area is referred to as the *distributed source* D_s. Load density function $\rho(x, y)$ determines the total rate of traffic generated inside any closed contour within D_s which must be transmitted to the destination. Hence, the rate of traffic generated inside a closed contour $a \subset D_s$ which is denoted by $w(a)$ is equal to

$$w(a) = \int_a \rho(x, y) \mathrm{d}x\mathrm{d}y$$

Let A denote the area including the distributed source and the destination where sensor nodes are deployed to carry the traffic from the source to the destination. The value of load density function is defined to be zero for the region between the distributed source and destination. Also, since all the traffic generated in the network needs to be sent to the destination, the value of $\rho(x, y)$ at the destination can be defined as a Dirac delta function with weight $-w_0$, where $w_0 = \int_{D_s} \rho(x, y) \mathrm{d}x\mathrm{d}y$.

The information flow field, denoted by $\vec{D}(x, y)$, is a vector field with two components (magnitude $|\vec{D}(x, y)|$ and direction $\vec{Dir}(x, y) = \frac{\vec{D}(x,y)}{|\vec{D}(x,y)|}$) at each point $(x, y) \in A$. $\vec{Dir}(x, y)$ represents the direction of flow of traffic at point (x, y), and magnitude $|\vec{D}(x, y)|$ represents the total amount of traffic passing per unit length of a line segment perpendicular to $\vec{Dir}(x, y)$. This implies that for any closed contour

$c \subset A$,

$$\oint_c \vec{D}(x,y) \cdot \mathrm{d}\vec{n} = \int_{S(c)} \rho(x,y)\mathrm{d}x\mathrm{d}y, \tag{2.1}$$

where $\mathrm{d}\vec{n}$ is an outgoing differential normal vector to the boundary of c, and $S(c)$ is the area surrounded by closed contour c. Equation (2.1) is similar to Gauss' law in electrostatics, and can also be expressed in the form of the following partial differential equation:

$$\nabla \cdot \vec{D}(x,y) = \rho(x,y) \tag{2.2}$$

It must be noted that although we have assumed that the information sink is located at a point in the network, according to (2.1), non-zero dimensions must be chosen for the destination in order to avoid the magnitude of information flow to grow to infinity as it gets closer to the sink. Choosing non-zero dimensions for data sink is also in accordance with networks where multiple antennas are located at a circle with non-zero radius around the sink.

In addition to equation (2.2), the information flow satisfies the Neumann boundary condition

$$\vec{D}_n(x,y) = 0, \quad \forall (x,y) \in \partial A, \tag{2.3}$$

where $\vec{D}_n$ is the normal component of $\vec{D}$ on the boundary of A, denoted by ∂A. This constraint forces the information flow to stay within the network geometry

without violating the boundaries. In reality, there are no sensors deployed outside of A; hence, no traffic passes through ∂A.

The above constraints on the flow field imply that for every location (x, y) inside A there exists a path from that point to the destination, which can be found by integrating the flow streamline from (x, y) all the way to the sink. Therefore, the information flow field represents a set of paths for transmitting traffic from the distributed source to the destination, which are not constrained by the location of sensor nodes.

Although the flow field satisfies equations (2.2) and (2.3), $\vec{D}(x, y)$ is not uniquely specified by these constraints. In a particular application, the flow field may be obtained from engineering knowledge. Alternatively, it may be obtained as a solution to an optimization problem. Later in this chapter, we suggest additional conditions to place on $\vec{D}$ such that the resulting vector field generates a desirable set of paths for traffic transmission to the sink.

Given a time-invariant vector field $\vec{D}(x, y)$, flow flux lines (also called streamlines) of $\vec{D}$ from each location (x, y) in the network to the destination can be found by solving the following Ordinary Differential Equation (ODE),

$$\frac{\mathrm{dX}(t)}{\mathrm{d}t} = \vec{D}(\mathrm{X}(t)), \tag{2.4}$$

where t is the integration variable and is not to be confused with time. Therefore, each streamline can be represented parametrically from the source to the destination by $f(t) = (x(t), y(t); x_0, y_0)$ for $t_0 \leq t \leq t_1$, where $x_0 = x(t_0)$ and $y_0 = y(t_0)$ refer

to the starting point of the streamline on the boundary of the distributed source and $x_1 = x(t_1)$ and $y_1 = y(t_1)$ refer to the corresponding landing point on the destination.

Later in this work, we consider network scenarios where the flow field scales linearly to infinity; i.e., we study networks with flow field $\vec{D}(x, y) = \theta\vec{D}_1(x, y), \forall(x, y) \in A$, where $\vec{D}_1$ is a given initial field and $\theta \in \mathbb{R}^+$. Note that by scaling the flow field as such the trajectory of flow streamlines does not change; however, the bounds of the parametrization variable t changes with the scaling factor θ. This can be mathematically represented as $f^\theta(t) = f^1(\theta t)$, where $f^\theta(t)$ is the parametric representation of a flow streamline of $\theta\vec{D}_1$. This is better understood by considering velocity fields; as the scaling factor θ increases, the trajectory of a flow streamline remains the same, however it is traversed faster.

Note that we have used the term flow streamlines interchangeably with flow flux lines throughout this work.

2.3 *p-norm* Flow Optimization

One important challenge in optimizing information flow flux lines is to decide what additional conditions to place on $\vec{D}$ such that the resulting vector field generates a desirable set of paths.

In [1] and [2], Kalantari and Shayman introduced a quadratic cost function of the information flow vector field $\vec{D}$ with the intuition of distributing traffic flow throughout the network. The quadratic cost function together with the constraints

on $\vec{D}$ results in the following optimization problem

$$\begin{aligned} \text{minimize} \quad & \int_A |\vec{D}(x,y)|^2 \mathrm{d}x\mathrm{d}y \\ \text{subject to} \quad & \nabla \cdot \vec{D}(x,y) = \rho(x,y) \\ & \vec{D}_n(x,y) = 0, (x,y) \in \partial A, \end{aligned} \tag{2.5}$$

which is a convex problem. They further proved that the optimal solution of (2.5) must have zero curl; i.e.,

$$\nabla \times \vec{D} = 0.$$

Now the combination of the zero-curl property, together with the divergence property and the boundary constraint uniquely specify the optimal flow field $\vec{D}$.

The motivation behind using a quadratic cost function was to disperse traffic in the network. This can increase the overall network throughput by reducing the interference among sensor nodes. However, quadratic optimization does not achieve maximum load balancing in the network. Therefore, we consider the following generalization of the quadratic optimization problem

$$\begin{aligned} \text{minimize} \quad & \int_A |\vec{D}(x,y)|^p \mathrm{d}x\mathrm{d}y \\ \text{subject to} \quad & \nabla \cdot \vec{D}(x,y) = \rho(x,y) \\ & \vec{D}_n(x,y) = 0, (x,y) \in \partial A, \end{aligned} \tag{2.6}$$

in which $p > 1$. Increasing p causes the optimization problem to increase spatial spreading in the network.

Note that by raising the cost function to power $\frac{1}{p}$, the optimal solution of (2.6) will not change; however, the new cost function will be the *p-norm* of the information flow $\vec{D}$. Hence, we call the generalized optimization problem (2.6) the *p-norm* flow optimization problem. As shown in [4], *p-norm* flow problem is a convex problem. This is proved by showing that the Hessian of $|\vec{D}(x,y)|^p$ is a positive definite matrix for $p > 1$.

The load balancing property of the *p-norm* problem is quite evident from its cost function. Consider the value of $|\vec{D}(x,y)|$ which can be assumed to be constant in a small neighborhood around (x,y). Now, if we double $|\vec{D}|$, it will affect the cost function by a factor of 2^p. Hence, the optimization problem tries to spread the traffic more uniformly as p grows from 1 to ∞.

2.4 Numerical Analysis of the *p-norm* Problem

Although the *p-norm* problem turned out to be a convex optimization problem, finding a closed form solution in general is not as easy as solving the quadratic optimization problem. Therefore, we numerically solve the *p-norm* problem using the optimization toolbox of MATLAB, and confirm its load balancing property.

Specifically, we show through numerical analysis that when p is close to 1, routes tend to pass through geometric shortest paths from a source to a sink; this reduces the average transport delay but can overload links which lie on shortest

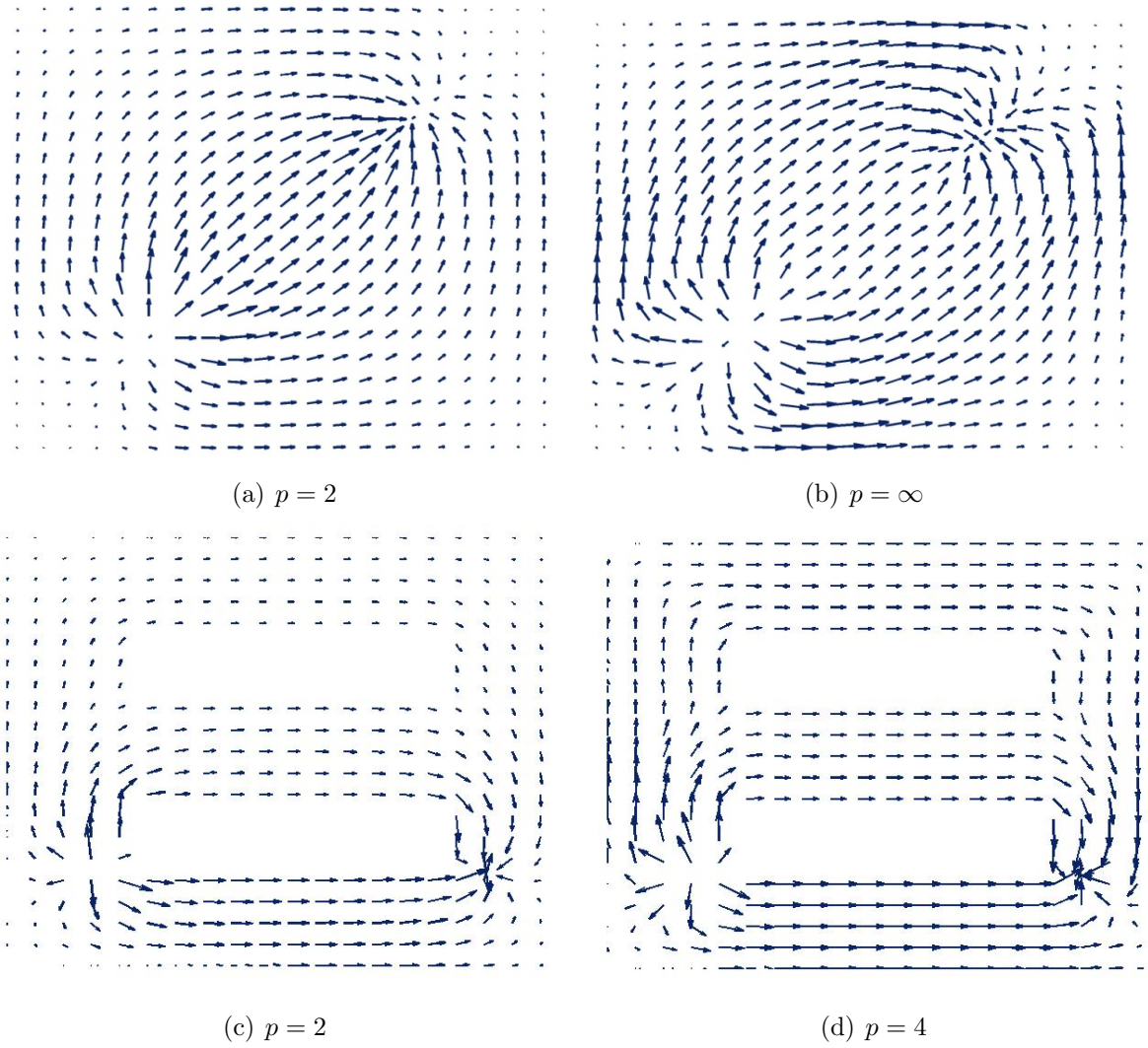

(a) $p = 2$ (b) $p = \infty$

(c) $p = 2$ (d) $p = 4$

Figure 2.1: Solving the *p-norm* problem for different values of p in different network topologies.

paths. By increasing the value of p from 1, the optimization tries to spread the traffic in the network, and as $p \to \infty$ the results achieve maximum load balancing. In practice, p can be selected based on a trade-off between delay and balancing the traffic over the network.

Fig. 2.1 shows the effect of load balancing as p increases in the *p-norm* problem numerically solved for two different network topologies.

2.4.1 Supporting Different Geometries

One of the issues in the *p-norm* flow optimization problem is the ability to support different geometries for the network to be deployed. Numerical PDE solvers may have different ways to handle this issue. The PDE toolbox of MATLAB, for example, has predefined matrices which must be filled in a special way to support different geometries. Moreover, numerical analyzers (including MATLAB) usually have Graphical User Interfaces (GUI) in which one can draw the desired geometry, and the predefined matrices will be filled indirectly. However, in order to discretize the constraints of the *p-norm* flow problem, numerical analyzers approximate the divergence operator with difference equations. This confines us to have plaid geometries [1]. This section presents an alternative way with which we can support any desired geometry while using rectangular geometries.

Consider the following flow optimization problem which is a more general

[1] A network of uniformly spaced squares that divides a geometry into units.

version of problem (2.6):

$$\begin{aligned} \text{minimize} \quad & \int_A k(x,y)|\vec{D}(x,y)|^p \mathrm{d}x\mathrm{d}y \\ \text{subject to} \quad & \nabla \cdot \vec{D}(x,y) = \rho(x,y) \\ & \vec{D}_n(x,y) = 0, (x,y) \in \partial A \end{aligned} \tag{2.7}$$

The only difference between problem (2.7) and (2.6) is in the existence of a $k(x,y)$ factor in the cost function of the optimization problem. Let $k(x,y)$ be a positive scalar weight function on A, taking a high value in parts of the rectangular geometry where no routes are desired to pass, and a relatively small value in places where we want the actual network to be. Therefore, $k(x,y)$ takes a small value inside the desired geometry and a relatively high[2] value in the undesired parts. In this way, the optimization problem forces the routes to stay within the desired geometry since passing through the undesired parts will drastically increase the cost.

As an illustrative example, consider Fig. 2.2(a) which shows the result of a 2-*norm* flow optimization problem in a polygon with a hole inside. As mentioned earlier, the network geometry can be defined in two ways; one way is to draw the desired geometry directly using a GUI, as shown in Fig. 2.2(b). The other way is to use problem (2.7) and suitably assign values to $k(x,y)$ in order to determine a network geometry within a rectangle, as shown in Fig. 2.2(c). In both Fig. 2.2(b) and 2.2(c), the real boundaries are specified by solid lines. The dashed lines in Fig. 2.2(c) are dummy boundaries which are drawn to specify our desired geometry.

[2]Theoretically, $k(x,y)$ must be equal to infinity in the undesired parts; however, keeping a ratio of 10^3 to 10^4 from its value in the desired parts is sufficient for the sake of numerical analysis.

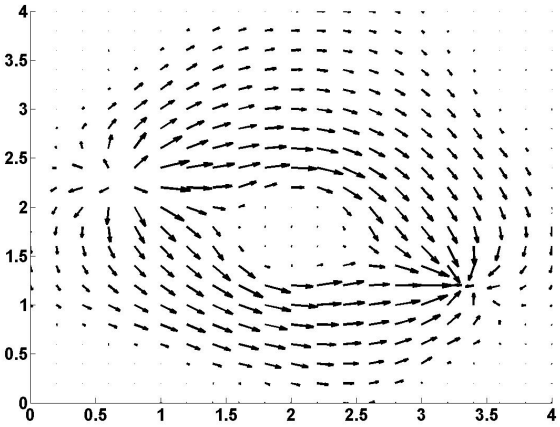

(a) Optimized information flow

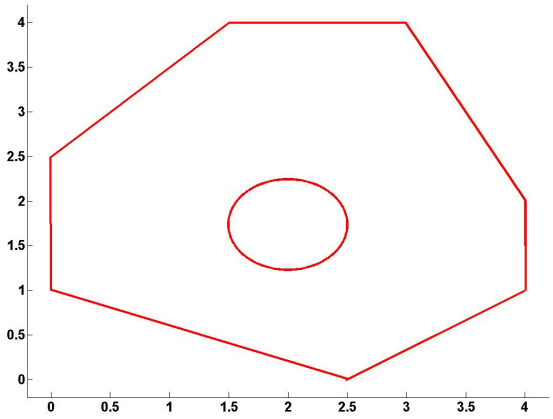

(b) Case I

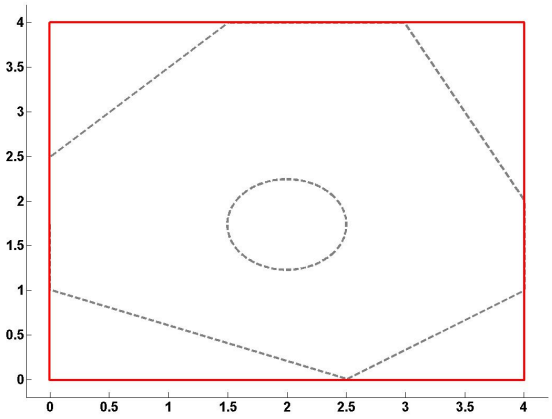

(c) Case II

Figure 2.2: 2-*norm* flow optimization problem. Case I: Defining the geometry through a GUI. Case II: Defining the geometry using the $k(x, y)$ factor.

The area between the solid and dashed lines and inside the inner circle are parts with a high k factor. The flow diagram related to Fig. 2.2(c) has small dots within the rectangle but outside the desired geometry which represent points with zero information flow. These are the points with a relatively high k factor residing in parts of the network geometry where no traffic is desired to pass through.

2.5 Summary

In this chapter, we presented an overview of the definition of information flow vector field, and briefly pointed out the constraints it must satisfy in order to model flow of traffic in a general network. We also overviewed the *p-norm* problem that places additional conditions on the flow field such that the resulting vector field generates a desirable set of paths for flow of traffic from the source to the destination.

In the second part of this chapter, we presented a numerical analysis of the *p-norm* flow optimization problem and discussed the different issues of the numerical analysis. Specifically, since numerical analyzers compute the divergence only on plaid geometries, we presented a modified *p-norm* flow problem where any desired geometry can be supported simply by assigning different values to a scalar factor $k(x, y)$.

Chapter 3

Topology Control in Large-Scale WSNs: (I) Inside the Distributed Source

3.1 Overview

3.1.1 Motivation

As stated throughout the work, our focus is on monitoring applications where sensor nodes deployed inside a distributed source D_s send periodic reports to the destination, which is located far away from the sensor nodes. We refer to the closure of the area with positive load density function as the distributed source.

Nodes inside the distributed source monitor (sense) the region and forward the traffic generated from other sensor nodes in the region. Hence, they must provide both coverage and connectivity. On the other hand, nodes outside the distributed source must only relay the traffic generated at the distributed source to the destination. Therefore, nodes outside the distributed source must be connected such that all the traffic generated in the source can be relayed to the destination. Coverage is not an issue for nodes inside this area. The required density of nodes in the area between the distributed source and destination is studied in the next chapter.

This chapter concentrates on the study of required density of nodes inside the distributed source so that the whole area is covered and that the active set of nodes

constitute a connected set such that all the traffic generated inside the source can be forwarded to the boundary of this region.

It has been concluded in the literature [32] that for monitoring applications where data is periodically transmitted to the sink, hierarchical routing protocols are the most efficient method. This is due to the excessive number of sensor nodes required due to random deployment which generates significant amount of redundant data that can be aggregated along the routes to the sink, thus reducing traffic and saving energy [31]. Clustering not only helps in reducing the amount of redundancy in data traffic, but also provides a means to study coverage of the distributed source.

We concentrate on a circular area with uniform load density function ρ. The circular region is divided into smaller clusters such that the whole area is covered and that nodes inside each cluster are responsible to forward C bps, which is equal to the transmission capacity of sensor nodes. In order to satisfy throughput requirements of the distributed source, density of sensor nodes randomly deployed in the region must be such that there exists at least one node inside each cluster. Let $|\vec{D}(l)|$ denote the traffic flux per unit length passing through a closed contour of radius l. Then, we show that a density of $n(l) = O(|\vec{D}(l)|^2)$ nodes is not sufficient to provide coverage while satisfying throughput requirements of the distributed source. On the other hand, we show that a density of $n(l) = O(|\vec{D}(l)|^2 \log |\vec{D}(l)|)$ nodes can cover the whole area while sensor nodes can forward the traffic in a uniform pattern to the boundary of the circular region.

3.1.2 Related Work

Due to versatility of subjects studied in this work, related works on each topic is investigated separately.

3.1.2.1 Coverage and Connectivity

One important issue that arises in WSNs is density control. Density control ensures only a subset of sensor nodes operate in the active mode, while fulfilling coverage and connectivity [33].

The coverage problem studies the minimum set of nodes that can cover the entire area to be monitored, based on a model for sensor nodes to monitor their neighboring region. Connectivity of the sensor nodes (to relay the collected traffic) can be studied in conjunction with the coverage problem if under some conditions, connectivity implies coverage or vice versa.

Assume that each sensor node can monitor an area of radius r_s (referred to as the sensing radius) from itself, and that each node can communicate with nodes residing within its transmission radius r_t. Then, in a homogeneous scenario, authors in [33, 34] have independently shown that if the transmission radius r_t of sensor nodes is at least twice of their sensing radius r_s, a complete coverage of a convex area implies connectivity among the working set of nodes.

Analysis of coverage and connectivity of sensor nodes in a WSN under different node deployment strategies and based on different coverage and communication models have been vastly studied in the literature. See [37] for more information in

this regard.

3.1.2.2 Clustering Techniques in WSNs

Clustering in WSNs involves grouping nodes into clusters and electing a cluster head (abbreviated as CH) such that nodes inside a cluster can directly communicate with their CH, and that each CH can forward the aggregated data to the data sink through other CHs [36].

Most of clustering protocols assume uniform cluster sizes throughout the network. However, due to the many-to-one nature of communications in WSNs, CHs closer to the sink forward more traffic than those farther away. Hence, the amount of traffic forwarded by different CHs is highly skewed. Shu et al. [35] studied the problem of cluster size assignment and proposed a scheme to decrease the cluster sizes as they get closer to the data sink.

Some of the other challenges in this area of research are discussed in [36]. In this work, we study suitable selection of transmission radii of nodes to ensure feasibility of inter and intra cluster communications. We also study the problem of cluster size selection to avoid skewed load distribution on CHs.

3.1.2.3 Tier-Based Routing Inside a Circular Area

Due to high density of sensor nodes in WSNs, it is not possible to build a global addressing scheme and assign one routing address per node in such networks. Different routing strategies to meet this specific need of WSNs have been widely

studied in the literature. Here, we briefly mention two of such routing protocols, namely AIMRP and DGRAM which are fully described in [5] and [6], respectively.

AIMRP (Address-light, Integrated MAC and Routing Protocol) is an integrated MAC and routing mechanism designed specifically for WSNs with (rare) event detection and reporting application. AIMRP is an address-light protocol which does not use strict per-node identifiers. At each hop, the node containing a packet indicates its tier number in the packet so that another node with a lower tier number can receive the packet. In this way, routing can be done by addressing at the tier level [5].

Authors in [6] propose another tier-based energy-efficient integrated MAC and routing protocol, called Delay Guaranteed Routing and MAC (DGRAM) protocol, which uses slot reuse technique to reduce the latency between two successive medium accesses by a sensor node. The proposed slot allocation strategy does not require exchange of control messages, which makes the deployment self-configuring.

DGRAM requires the sensor nodes to be deployed with uniform density throughout the network region. Slot assignments in DGRAM happen in three levels of hierarchy: tier level, block level and node level. Hence, it is not suitable for WSNs with high density. Also, certain requirements of sensor networks (such as coverage) are not considered in this work. Nonetheless, the slot assignment technique used in [6] has been inspiring to this work.

3.2 Network Model and Assumptions

Consider the distributed source to be a circular area of radius $R = 1$ with uniform load density function $\rho(x, y) = \rho$. Sensor nodes are assumed to be able to change their transmission radius r_t by suitably changing their transmission power as a function of their distance to the center. This should be done in order to reduce the amount of interference on neighboring nodes while maintaing network connectivity. Sensing regions are also assumed to be circular; i.e., each sensor node can monitor an area of radius r_s around itself. Furthermore, sensor nodes are assumed to have a transmission capacity of C bps.

Using the divergence property of information flow vector field and symmetry of the problem, magnitude of information flow inside the circular area has the following relation:

$$|\vec{D}(l)| = \frac{1}{2}\rho l, \quad 0 \leq l \leq R \tag{3.1}$$
$$\phi \in [0, 2\pi),$$

where (l, ϕ) represent the polar coordinates of a point from the center of the circular area. The flow field is also assumed to be irrotational, and hence the direction of information flow is radially outward toward the boundary of the circular region.

3.3 Partitioning the Distributed Source

To study the required density of nodes that cover D_s and propose a hierarchical routing protocol, the network is decomposed into tiers and each tier is divided into different clusters. This is shown in Fig. 3.1. Nodes within each cluster are responsible to collect data from the region inside the cluster and send their data to the CH. CH collects data and relays the traffic to a neighboring cluster in the next tier toward the boundary, after performing some sort of data aggregation. CHs in each tier are responsible to collect data as well as relay the traffic received from inner tiers; hence, due to uniform transmission capacity of nodes, the width of tiers and the size of clusters must reduce as they get closer to ∂D_s. In order to reduce the amount of interference on neighboring clusters due to concurrent transmissions, the transmission radius of nodes must also reduce proportional to the size of their clusters.

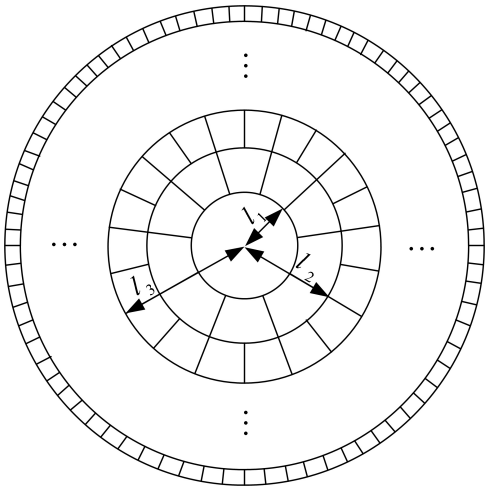

Figure 3.1: Partitioning the area of the distributed source into clusters.

Let $l_i, i = 1, 2, \cdots$ denote the radius of different tiers, where the first tier is

the disk of radius l_1 at the center, and the ith tier ($i > 1$) is the belt region confined between circles of radius l_{i-1} and l_i. Tiers are further divided into clusters such that each CH is responsible to transmit a total traffic of C bps. Let $N(i)$ denote the required number of clusters at the ith tier; then,

$$N(i)C = \rho\pi l_i^2 \tag{3.2}$$

Also, since the first tier is a disk around the center, l_1 can be chosen such that $N(1) = 1$; hence, $l_1 = \sqrt{\frac{C}{\pi\rho}}$.

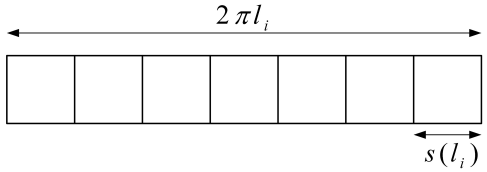

Figure 3.2: ith tier shown as a rectangle ($i \geq 2$).

Fig. 3.2 shows a tier for ($i \geq 2$) where the belt shape of the tier is approximated as a rectangle of length $2\pi l_i$ and width $s(l_i)$ which denotes the size of square clusters at the ith tier. Therefore,

$$N(i)s(l_i) = 2\pi l_i, \text{ for } i \geq 2 \tag{3.3}$$

Using relation (3.2) and substituting $s(l_i) = l_i - l_{i-1}$ in (3.3), the following recursive

relation is derived:

$$\begin{aligned} l_i(l_i - l_{i-1}) &= \frac{2C}{\rho}, \text{ for } i \geq 2 \\ \text{and } l_1 &= \sqrt{\frac{C}{\pi\rho}} \end{aligned} \tag{3.4}$$

Hence, l_i can be calculated as follows:

$$\begin{aligned} l_i &= a_i\sqrt{\frac{C}{\pi\rho}}, \text{ for } i \geq 1, \\ \text{where} & \\ 2a_i &= a_{i-1} + \sqrt{8\pi + a_{i-1}^2}, \text{ for } i \geq 2, \\ \text{and } a_1 &= 1 \end{aligned} \tag{3.5}$$

Also, from relations (3.2) and (3.3), the width of each tier is equal to

$$\begin{aligned} s(l_i) &= \frac{2C}{\rho}\frac{1}{l_i}, \text{ for } i \geq 2 \\ &= \frac{2\pi}{a_i}l_1 \end{aligned} \tag{3.6}$$

The following properties of the sequence $\{a_i\}_{i=1}^{\infty}$ will be found useful for the rest of the analysis.

Lemma 3.1: The sequence $\{a_i\}_{i=1}^{\infty}$ which is generated based on the recursive relation (3.5) has the following properties:

1. $a_{i+1} < a_i + \sqrt{2\pi}$

2. $\{\frac{a_{i+1}}{a_i}\}_{i=1}^{\infty}$ is a decreasing sequence and $\lim_{i\to\infty} \frac{a_{i+1}}{a_i} = 1$.

Proof of the above statements are left for the reader.

3.4 Required Density of Nodes

Based on the previous discussion, in order to meet the throughput requirement of the circular region, density of sensor nodes must be such that there exists at least one node inside each cluster. Moreover, for CHs to cover the whole area of their corresponding clusters, sensing radius of nodes must be chosen such that

$$\begin{aligned} r_s(l_i) &= \sqrt{2}s(l_i), \text{ for } i \geq 2, \\ \text{and } r_s(l_1) &= 2l_1 \end{aligned} \tag{3.7}$$

Hence, using relations (3.6) and (3.7), sensing radius of nodes is inversely proportional to the distance from the center of the circular region.

The following lemma investigates the necessary and sufficient relation between the sensing radius and the transmission radius of nodes such that network coverage and connectivity requirements are satisfied simultaneously.

Lemma 3.2: The necessary and sufficient condition to guarantee connectivity at the cluster level while maintaining coverage of the distributed source D_s is met when $r_t(l) = k_0 r_s(l)$, for some $\sqrt{2} \leq k_0 \leq 2$.

Proof. Connectivity at the cluster level is defined as existence of a path between any two CHs in the network. To ensure connectivity at the cluster level, neighboring

clusters at consecutive tiers and adjacent clusters inside each tier must be connected. Fig. 3.3 and Fig. 3.4 depict worst case scenarios for connectivity of CHs inside neighboring clusters at the same and at two consecutive tiers, respectively.

From Fig. 3.3, $r_t(l_i) \geq 2s(l_i) = \sqrt{2}r_s(l_i)$ is a necessary condition to connect two adjacent clusters in the same tier. Also from Fig. 3.4, $r_t(l_i) = 2r_s(l_i)$ is sufficient to guarantee connectivity of CHs in neighboring clusters at consecutive tiers. Hence, for a given sensing radius r_s, the necessary and sufficient transmission radius to provide cluster level connectivity is equal to $r_t(l) = k_0 r_s(l)$ for some $\sqrt{2} \leq k_0 \leq 2$. We assume $r_t(l) = 2r_s(l)$ for the rest of the analysis. □

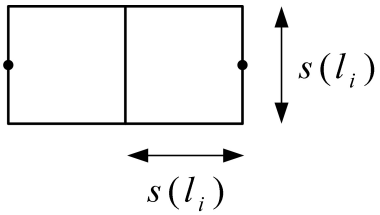

Figure 3.3: $r_t(l) = \sqrt{2}r_s(l)$ to guarantee connectivity of adjacent clusters in the same tier.

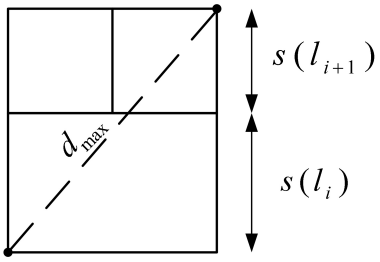

Figure 3.4: $r_t(l_i) = 2r_s(l_i)$ is sufficient to guarantee connectivity of CHs in neighboring clusters at consecutive tiers.

Remark 1: Note that the exact value of k_0 does not play an important role in our analysis since it does not change the order of required number of nodes.

In the rest of this section, we perform an asymptotic analysis to derive the required density of nodes that ensure network coverage as $\rho \to \infty$.

Based on equations (3.6) and (3.7), $r_s(l) = \frac{2\sqrt{2}C}{\rho l}$, for $0 < l \leq R$; hence,

$$r_s(l) = \frac{\sqrt{2}C}{|\vec{D}(l)|} \tag{3.8}$$

Therefore, the sensing radius (and hence the transmission radius) of nodes are inversely proportional to the magnitude of information flow everywhere in the distributed source.

Let $n(l, \phi)$ represent the required density of sensor nodes as a function of location in D_s. Due to the existing symmetry in the problem, the required density of nodes is not a function of ϕ; hence, $n(l, \phi) = n(l)$.

The following lemma is used in the proof of the theorems stated in the rest of this work.

Lemma 3.3:

$$\exp(-\frac{p}{1-p}) < 1 - p < \exp(-p), \text{ for } |p| < 1 \tag{3.9}$$

Proof. The inequality in the right hand side can be easily verified by comparing $1 - p$ to the Taylor expansion of $\exp(-p)$ around the origin. For the inequality in

the left hand side, proceed as follows:

$$\begin{aligned} 1-p &= \exp\Big(\log(1-p)\Big), \text{ where} \\ \log(1-p) &= -\sum_{i=1}^{\infty}\frac{1}{i}p^i \\ &\geq -\sum_{i=1}^{\infty}p^i = -\frac{p}{1-p}, \text{ for } |p|<1. \quad \square \end{aligned}$$

Theorem 3.1: A random deployment of sensor nodes with density $n(l) = O(|\vec{D}(l)|^2)$ is not sufficient to cover D_s while satisfying the traffic requirements of the distributed source.

Proof. Assume that sensor nodes with density $n(l) = O(|\vec{D}(l)|^2)$ are randomly deployed inside D_s. Hence, a total number of $n(l)2\pi ls(l)$ nodes is distributed uniformly at random within the tier of distance l from the center. Based on equations (3.2) and (3.3), the tier is partitioned into $N(l) = \frac{\pi l^2}{C}\rho$ square clusters of size $s(l) = \frac{2C}{l}\frac{1}{\rho}$. Let P_d denote the probability that D_s is not covered, and $\Upsilon_j(l)$ be the event that no sensor nodes exist in jth cluster $C_j(l)$, $j = 1, \cdots, N(l)$, of the tier at distance l from the center.

$$\begin{aligned} P_d &> P[C_j(l) \text{ not covered } |\Upsilon_j(l)]P[\Upsilon_j(l)] \\ &= P[C_j(l) \text{ not covered } |\Upsilon_j(l)](1-\frac{1}{N(l)})^{n(l)2\pi ls(l)} \\ &> P[C_j(l) \text{ not covered } |\Upsilon_j(l)]\exp\Big(-\frac{n(l)2\pi ls(l)}{N(l)}\frac{1}{1-\frac{1}{N(l)}}\Big), \end{aligned}$$

where the second line is derived based on the uniform distribution of nodes within

the tier, and the third line is derived using Lemma 3.3. Now, by substituting $n(l) = k|\vec{D}(l)|^2 = k\frac{l^2}{4}\rho^2$, for some $k > 0$, and taking the limit as $\rho \to \infty$,

$$P_d \;>\; P[C_j(l) \text{ not covered } |\Upsilon_j(l)] \exp(-kC^2) \tag{3.10}$$

The first term in the right hand side of (3.10) has a strictly positive probability, and the exponential term is also strictly positive for any positive real k; hence, $P_d > 0$. □

Theorem 3.2: A random deployment of sensor nodes with density $n(l) = O(|\vec{D}(l)|^2 \log |\vec{D}(l)|)$ is sufficient to cover the distributed source and to forward the traffic generated inside D_s to its boundary.

Proof. The proof of this theorem has two steps; first, we show that $n(l)$ covers the whole area of D_s. Next, we show that the traffic generated inside the circular region can be forwarded to ∂D_s. The latter is shown by proposing a feasible controlled access scheme.

1. Meeting the coverage requirement: As mentioned earlier, for any finite ρ, the distributed source is partitioned into tiers of width $s(l_i)$ such that $\sum_{i=1}^{m(\rho)} s(l_i) = 1$, where $m(\rho)$ denotes the total number of tiers. Using equation (3.6), the relation between m and ρ can be stated more explicitly through the following series,

$$\sum_{i=1}^{m(\rho)} \frac{1}{a_i} = \frac{1}{2\sqrt{\pi C}} (\rho)^{\frac{1}{2}}$$

The above relation shows that m is an increasing function of ρ.

For each ρ, let $\{C_{i,j},\ i=\ 1,\cdots,m(\rho)\ \ j=\ 1,\cdots,N(i)\}$ be the set of clusters partitioning the whole area of the distributed source. Accordingly, define $\Upsilon_{i,j}$ to be the event $\{C_{i,j}$ is empty$\}$. Now,

$$\begin{aligned} P[D_s \text{ is covered}] &> P[\bigcap_{i,j} \Upsilon_{i,j}^c] \\ &= 1 - P[\bigcup_{i,j} \Upsilon_{i,j}] \\ &\geq 1 - \sum_{i=1}^{m(\rho)} \sum_{j=1}^{N(i)} P[\Upsilon_{i,j}], \end{aligned} \tag{3.11}$$

where $\Upsilon_{i,j}^c$ is the complement of $\Upsilon_{i,j}$. As $\rho \to \infty$, the double series in the last line of (3.11) can be written in the integral form below

$$\begin{aligned} \lim_{\rho\to\infty} \sum_{i=1}^{m(\rho)} \sum_{j=1}^{N(i)} P[\Upsilon_{i,j}] &= \int_{l=0}^{1} \sum_{j=1}^{N(l)} P[\Upsilon_j(l)]\mathrm{d}l \\ &= \int_0^1 N(l)\Big(1 - \frac{1}{N(l)}\Big)^{n(l)2\pi l s(l)}\mathrm{d}l \\ &\leq \int_0^1 N(l)\exp\Big(-\frac{n(l)2\pi l s(l)}{N(l)}\Big)\mathrm{d}l, \end{aligned}$$

and as $\rho \to \infty$, for $n(l) = k|\vec{D}(l)|^2 \log|\vec{D}(l)|$,

$$= \frac{\pi 2^{kC^2}}{C}\rho^{(1-kC^2)} \int_0^1 l^{2-kC^2}\mathrm{d}l, \tag{3.12}$$

which goes to zero for $\frac{1}{C^2} \leq k \leq \frac{2}{C^2}$, making the double series in (3.11) vanish as $\rho \to \infty$; hence, the network is covered. Note that although the integral in the last line of (3.12) is not defined for $k > \frac{2}{C^2}$, but if the network is covered

with $n(l) = k_1|\vec{D}(l)|^2 \log|\vec{D}(l)|$ for $\frac{1}{C^2} \leq k_1 \leq \frac{2}{C^2}$, then it is also covered for any $k > k_1$.

2. Meeting the traffic flow requirement: In this part, we show that a TDMA-based integrated MAC and routing scheme with finite number of slots per each time frame can be applied to the network to carry all the traffic generated inside the distributed source to its boundary. Slot assignments in our proposed scheme happen in two levels of hierarchy: tier level and cluster level.

   (i) Tier level: at this level we need to show that tiers can be partitioned into groups of N_s tiers (N_s bounded and independent of ρ) such that concurrent transmissions of nodes inside tiers $kN_s, k \geq 1$ apart do not interfere with each other.

   Let us start with a simple case where nodes distributed throughout the circular region have uniform sensing (and transmission) radius, and that the tiers around the center are of equal width as well. This case was studied in [6] with uniform tier width αr_t. For this example, it can be easily derived that $N_s = \frac{2r_I}{\alpha r_t} + 1$, where the first term assures that interference zones of concurrent transmitters do not interfere with each other and the additional term takes into account cases where transmitters are on the edge of their corresponding tiers. This is further shown in Fig. 3.5.

   In our work, however, the transmission radius of nodes and the width of tiers are a function of distance from the center. Hence, N_s is also a function of distance from the center and that the maximum $N_s(i)$ must be chosen to

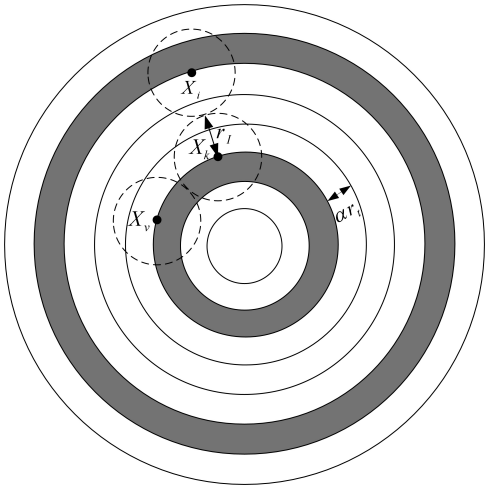

Figure 3.5: Nodes X_i and X_k in the shaded tiers have non-interfering interference zones and can transmit simultaneously. The same situation holds for X_k and X_v which are in the same tier.

implement a unique protocol for all nodes in the network. Furthermore, in the asymptotic analysis, another important challenge is to be able to choose a finite N_s independent of ρ which remains bounded as $\rho \to \infty$. Therefore, using the same methodology, in a non-uniform scenario $N_s(i)$ must be chosen such that

$$\sum_{j=i+1}^{i+N_s(i)-1} s(l_j) \geq r_I(l_i) + r_I(l_{i+N_s(i)}), \text{ for } i \geq 1$$

$$\text{hence, } \sum_{j=i+1}^{i+N_s(i)-1} \frac{1}{a_j} \geq 2\sqrt{2}q\left(\frac{1}{a_i} + \frac{1}{a_{i+N_s(i)}}\right) \tag{3.13}$$

Using Lemma 3.1, $a_{i+j} < a_i + j\sqrt{2\pi},$ for $i \geq 1$ and $j \geq 0$, and

$$\begin{aligned}
\sum_{j=i+1}^{i+N_s(i)-1} \frac{1}{a_j} &> \sum_{j=1}^{N_s(i)-1} \frac{1}{a_i + j\sqrt{2\pi}} \\
&> \int_1^{N_s(i)} \frac{1}{a_i + \sqrt{2\pi}x} \mathrm{d}x \\
&= \frac{1}{\sqrt{2\pi}} \ln\Big(1 + \frac{(N_s(i)-1)\sqrt{2\pi}}{a_i + \sqrt{2\pi}}\Big)
\end{aligned}$$

Now, if $N_s(i)$ is chosen such that

$$\begin{aligned}
\frac{1}{\sqrt{2\pi}} \ln\Big(1 + \frac{(N_s(i)-1)\sqrt{2\pi}}{a_i + \sqrt{2\pi}}\Big) &\geq 2\sqrt{2}q(\frac{1}{a_i} + \frac{1}{a_{i+N_s(i)}}) \\
&> 4\sqrt{2}q\frac{1}{a_i},
\end{aligned}$$

inequality (3.13) holds as well. Solving the above inequality for $N_s(i)$ gives,

$$N_s(i) \geq (1 + \frac{a_i}{\sqrt{2\pi}})\Big(\exp(\frac{8\sqrt{\pi}q}{a_i}) - 1\Big) + 1, \tag{3.14}$$

where the right hand side of (3.14) is a decreasing function of i and is also independent of ρ. Therefore, a finite N_s independent of ρ can be chosen to be $N_s = \max_i\{N_s(i)\} = N_s(1)$, which can be found using (3.14).

(ii) Cluster level: in order to have concurrent transmissions at each tier, clusters inside each tier must also get divided into N_c groups. Using the same communication protocol, in order to avoid significant interference, $2r_I(l) =$

$2q_I r_t(l) \leq (N_c - 1)s(l)$. Therefore,

$$N_c \geq \lceil 4\sqrt{2}q + 1 \rceil, \tag{3.15}$$

which is independent of l and ρ.

The above discussion shows that with applying a TDMA scheme with a frame size of $N_s N_c$ slots, the traffic generated inside D_s can be successfully forwarded to ∂D_s. $\square$

Relay of traffic from the distributed source to the destination can be done using any routing protocol which is designed to take care of the many-to-one nature of communications in WSNs. In particular, relay of traffic to the destination can be along flux lines of information flow vector field $\vec{D}(x, y)$. This is fully described in Chapter 4, where it is shown that the required density of sensor nodes to "follow" flow flux lines of an irrotational flow field $\vec{D}$ in the region between the distributed source and destination is again $O(|\vec{D}(x, y)|^2 \log |\vec{D}(x, y)|)$.

3.4.1 Uniform Flow of Traffic

Due to the existing symmetry in D_s, it is desired for CHs to forward traffic in a uniform pattern from one tier to the next. This also avoids the need for queueing. To do so, each cluster in the ith tier must be able to communicate with $\frac{\lceil N(i+1) \rceil}{\lceil N(i) \rceil} = \frac{\lceil a_{i+1}^2 \rceil}{\lceil a_i^2 \rceil}$ clusters in the $(i+1)$th tier. The value of this ratio is listed in Table 4.1 for $1 \leq i \leq 5$.

As shown in the table, $1 < \frac{\lceil N(i+1) \rceil}{\lceil N(i) \rceil} \leq 2$ for $i > 1$. This is because, based on Lemma 3.1, $\{\frac{a_{i+1}}{a_i}\}$ is a monotonically decreasing sequence reaching 1 (from the

Table 3.1: Number of clusters at each tier

i	a_i	$\lceil a_i^2 \rceil$	$\frac{\lceil N(i+1) \rceil}{\lceil N(i) \rceil}$
1	1	1	10
2	3.05	10	2
3	4.45	20	1.6
4	5.57	32	1.34
5	6.53	43	1.28

right side) in the limit. In order to reduce the complexity of routing and use a uniform ratio along different tiers, we manipulate the number of clusters at each tier by doubling the number of clusters moving from one tier to the next for $i \geq 2$; hence, we choose $\frac{N(i+1)}{N(i)} = 2$, for $i \geq 2$. Note that the width of each tier remains unchanged through this modification; however, the number of clusters at each tier will be at most double the required number of clusters for data aggregation and forwarding which was derived in (3.2). Hence, the shape of clusters change from squares to rectangles. Using same sensing and transmission radii as before, none of the previously derived asymptotic results change. To limit the effect of interference due to simultaneous transmissions, number of groups at cluster level (N_c) must get doubled to compensate for using more clusters in each tier. The partitioning shown in Fig. 3.1 was done based on this assumption.

The maximum distance between two nodes communicating based on the above routing protocol is shown in Fig. 3.4 and is calculated below (for $i \geq 2$ where $\frac{N(i+1)}{N(i)} = 2$):

$$d_{max}^2 \leq \Big(2s(l_{i+1})\Big)^2 + \Big(s(l_i) + s(l_{i+1})\Big)^2, \tag{3.16}$$

where d_{max} denotes the maximum distance between nodes. Using the inequality $s(l_{i+1}) < s(l_i)$ in (3.16) (which can easily be derived from (3.6)), it is evident that $d_{max} < r_t(l_i) = 2\sqrt{2}s(l_i)$. Therefore, relay of traffic to the boundary of the circular area in a uniform pattern is possible.

3.5 Summary

In WSNs with monitoring applications, we modeled flow of traffic using a load density function. This provided a framework to better study open problems such as ensuring connectivity, computing optimal cluster sizes and density control in WSNs while meeting special requirements of such networks. In a circular region with uniform load density function, let $|\vec{D}(l)|$ denote the traffic flux per unit length passing through a closed contour of radius l. We showed that a density of $n(l) = O(|\vec{D}(l)|^2)$ nodes is not sufficient to provide coverage while satisfying throughput requirements of the distributed source. On the other hand, we showed that a density of $n(l) = O(|\vec{D}(l)|^2 \log |\vec{D}(l)|)$ nodes can provide coverage of the network region while forwarding the traffic to the boundary of the circular region in a uniform pattern. This was shown by proposing a feasible TDMA-based integrated MAC and routing scheme with finite number of slots per each time frame.

Chapter 4

Topology Control in Large-Scale WSNs: (II) Between the Distributed Source and Destination

4.1 Overview

4.1.1 Implementability: A New Notion of Connectivity

In this chapter, we study the required density of nodes to forward traffic along information flow field. We show that following the optimal paths for flow of traffic between the distributed source and the destination requires more nodes than providing network connectivity. To perform this analysis, a new notion of connectivity called implementability is defined which represents the ability of sensor nodes to forward traffic along flux lines (also referred to as flow streamlines) of a known flow field as its magnitude scales linearly to infinity. Although the concept of implementability is defined for a general flow vector field, in this work we concentrate on studying flow fields which have zero divergence and zero curl in the region between the distributed source and destination. We refer to such flow fields as ideal flows. Note that based on the definition of information flow vector field, its divergence is zero in the region between the source and destination. However, the constraint of having zero curl confines the analysis to flow fields which are the solution of the 2-*norm* flow problem. The final results indicate that for a given ideal flow field

$\vec{D}(x,y)$, a density of $n(x,y) = O(|\vec{D}(x,y)|^2)$ sensor nodes is not sufficient to relay traffic along flow streamlines. This result contradicts the prior result of [10] where authors stated otherwise. On the other hand, we show that $\vec{D}(x,y)$ is implementable with a density of $n(x,y) = O(|\vec{D}(x,y)|^2 \log |\vec{D}(x,y)|)$ sensor nodes.

Note that previous results on connectivity have been obtained based on the implicit assumption of a routing protocol, capable of exhaustively searching all possible routes, between all pairs of nodes [14]. However, the tight limitation of energy in sensor networks calls for a lightweight protocol stack. We propose a joint MAC and routing protocol which requires no more than $n(x,y) = O(|\vec{D}(x,y)|^2 \log |\vec{D}(x,y)|)$ nodes to relay traffic along flow streamlines. The proposed tier-based scheme also provides a framework to reduce the size of addressing fields (by requiring tier-level addressing instead of node-level addressing) and apply power-saving methods by using clustering techniques, and hence meeting the specific requirements of dense sensor networks. The details of addressing and clustering techniques should be specified based on network geometry and are out of the scope of this work.

4.1.2 Related Work

A vector field representation for flow of traffic in WSNs was first introduced in [1, 2] with inspiration from electrostatics. Approaches based on electrostatics have become popular thereafter. [10], [29], [16], and [15] are among the works based on this analogy.

The spatial distribution of wireless nodes that can transport a given volume

of traffic in a sensor network was first studied in [10]. Under a general assumption on the physical and medium access control (MAC) layers, the authors showed that the optimal distribution of nodes induces a traffic flow identical to the electrostatic field that would exist if the sources and sinks of traffic were substituted by an appropriate distribution of electric charge. This result was based on the assumption that a location (x, y) with node density $n(x, y)$ can support an information flow with magnitude less than or equal to $\lambda\sqrt{n(x, y)}$ for some constant λ. In this work, we show that this assumption is not realistic under the new notion of connectivity and under more accurate communication protocols.

4.1.3 Summary of Results

First, a new notion of connectivity called implementability is defined which uses the magnitude and direction of information flow field to form an increasing set of disjoint regions such that, as magnitude of flow field scales linearly to infinity, traffic can be forwarded to the destination in a multihop fashion along the flow streamlines with constant rate inside each region. For the flow field to be implementable, density of sensor nodes must be such that piecewise linear routes can be formed w.h.p inside each region, as the scaling factor goes to infinity. We show that in the limit, the set of piecewise linear routes converges uniformly to a set of flow streamlines, which by definition are optimal paths for flow of traffic.

To perform the implementability analysis, we first consider a unit square example with uniform information flow parallel to the sides of the square and study

the required number of nodes to implement the flow field inside the square. We show that the results of this simple example can be extended to networks with more complicated geometries using a flow-based curvilinear coordinate system which partitions the network into smaller approximately square grids with flow streamlines similar to the unit square network. The existence of such coordinate system can be shown for flow fields which have zero divergence and zero curl in the region between the source and destination, and hence the implementability analysis is confined to such flow fields in this work.

For the unit square example with uniform flow field $\vec{D}^{(l)}$, we first show that a quadratic relation between density of nodes and $|\vec{D}^{(l)}|$ is not sufficient to implement the flow field. To show this, we prove that implementability requires more than simple connectivity by showing that a disconnected network of nodes cannot implement the flow field; i.e., the probability that an isolated node affects forming a piecewise linear route inside its associated region is strictly positive as $|\vec{D}^{(l)}| \to \infty$.

Next, we show that increasing the number of sensor nodes to $N = O(|\vec{D}^{(l)}|^2 \log |\vec{D}^{(l)}|)$ nodes is sufficient to implement the flow field. The sufficiency is shown by proposing a joint MAC and routing protocol which requires the same order of nodes to forward the traffic within each flow region using either the Protocol or Physical Model.

The main idea of the proposed scheduling scheme is to divide time and frequency domains into smaller slots and sub-channels such that transmissions at each time slot and frequency sub-channel abide by either of the communication models. The steps involved in this scheduling scheme are as follows:

- Tessellate the square into smaller square cells of proper width (proportional to the width of the flow regions).

- Divide cells into M^2 groups, for a fixed M to be specified later, such that at each time slot $m = 1, \cdots, M^2$, nodes inside the mth group can successfully forward traffic to their neighboring nodes, and

- Determine transmission power or transmission radius of nodes such that inter-cell communication is possible.

The proof is completed by showing that a finite M can be found under either communication model, and that w.h.p there exists at least one node inside each cell to forward the traffic in its associated time slot.

The proposed tier-based scheme provides a framework to reduce the size of addressing fields (by requiring tier-level addressing instead of node-level addressing) and apply power-saving methods by using clustering techniques. Highly optimized protocol stacks can be designed for different network geometries based on their specific properties; the details of addressing and clustering techniques are beyond the scope of this work.

4.2 Implementability of Information Flow Field

The goal of this chapter is to provide a means to study the required density of nodes to communicate in a multihop fashion along flow streamlines. Let C denote the transmission capacity of sensor nodes (measured in bps), and $0 < \gamma \leq 1$ be a parameter determined by the MAC protocol which represents the portion of time

and/or frequency bandwidth assigned to each node for data transmission. Hence, with w_0 referring to the total amount of traffic generated at the distributed source, a total number of $n_s(A) = \lceil \frac{w_0}{\gamma C} \rceil$ routes is required to relay all the traffic from the source to the destination.

For a known information flow $\vec{D}(x, y)$, a set of $n_s(A)$ flux lines can be selected to represent desired paths for flow of traffic. The set of flux lines can then be used to partition the area between the distributed source and the sink into a set of disjoint regions so that traffic can be relayed in a multihop fashion inside each region with constant rate. If density $n(x, y)$ of sensor nodes is high enough such that as $|\vec{D}|$ scales linearly to infinity piecewise linear routes can be formed inside each region to forward traffic to the destination, then the information flow field $\vec{D}$ is said to be implementable with node density $n(x, y)$.

To form piecewise linear routes, a set of $n_s(A)$ streamlines is chosen by placing flow seeds on the boundary of the distributed source and using relation (2.4) to integrate the flow lines all the way to the destination. By bisecting the region between each pair of streamlines, network geometry A is partitioned into $n_s(A)$ streamline regions. Each region is the area between a pair of bisections and includes a streamline in its interior. To avoid intersection of piecewise linear routes, they must stay within the margins of their corresponding streamline regions.

Consider a rectangular area with a set of flux lines passing through and parallel to the vertical sides of the rectangle, similar to Fig. 4.1. This resembles flux lines passing through a small enough area element inside A. Using the same method described above, the rectangular area is partitioned into a set of streamline regions

which in this case is a set of rectangular strips as shown in the figure. Sensor nodes are deployed inside the rectangle uniformly at random. In order for sensor nodes to be able to form piecewise linear routes inside each streamline region, the transmission radius of nodes must be less than the width of the narrowest strip[1]. Otherwise, routes might violate the margins of their corresponding streamline regions[2].

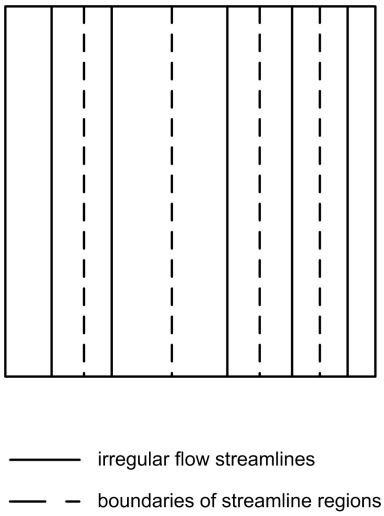

Figure 4.1: A set of irregular flow streamlines.

As transmission radius of nodes decreases, more nodes must be deployed to form routes inside each strip. This is because density of nodes must be such that each node can find another node within its transmission radius. Therefore, required density of nodes is minimized if flow flux lines are evenly spaced within the rectangle.

Following a similar argument, the set of $n_s(A)$ streamlines chosen in A must be "locally regular" in order to minimize the required number of nodes inside each area element. A more precise definition of local regularity is stated in the sequel.

[1]In order to ensure that the traffic inside each strip stays within itself, nodes inside adjacent strips must use different frequency sub-channels to carry traffic.

[2]More accurately, the transmission radius of nodes must be proportional to the width of the narrowest strip. The frequency channel must again be divided into sub-channels to conserve traffic within each streamline region.

Implementability analysis is an asymptotic approach and the probability of events are calculated as $|\vec{D}(x,y)|$ scales linearly to infinity. As it is proven in the following lemma, linear scale of the load density function $\rho(x,y)$ within the distributed source results in linear scale of the information flow vector field (when derived from the *p-norm* problem), everywhere in the network.

Lemma 4.1: Let $\vec{D}_1(x,y)$ denote the optimal solution of the *p-norm* problem in a region A with load density function $\rho_1(x,y)$. Then solving (2.6) for $\rho(x,y) = \theta\rho_1(x,y)$ results in $\vec{D}(x,y) = \theta\vec{D}_1(x,y)$.

Proof. Since the *p-norm* problem (2.6) is a convex optimization problem with differentiable objective and constraint functions, the KKT[3] conditions are necessary and sufficient for the optimal solution to be met. let $L(\vec{D},\nu_\theta)$ denote the Lagrangian function of the *p-norm* problem with $\theta\rho_1(x,y)$ load density function, and ν_θ denote the dual variable associated with the problem. Now, if $(\vec{D}_1,\nu_1^*)$ be the optimal primal and dual solutions of the problem with $\theta = 1$, then based on the KKT conditions,

$$\begin{aligned}\nabla_{\vec{D}} L(\vec{D}_1,\nu_1^*) = \quad & \nabla_{\vec{D}}\Big[\int_A |\vec{D}_1(x,y)|^p \mathrm{d}x\mathrm{d}y - \\ & \int_A \nu_1^*(x,y)\big(\nabla\cdot\vec{D}_1(x,y) - \rho_1(x,y)\big)\mathrm{d}x\mathrm{d}y\Big] = 0,\end{aligned} \tag{4.1}$$

and

$$\nabla\cdot\vec{D}_1(x,y) - \rho_1(x,y) = 0$$

Note that $\nabla_{\vec{D}}$ is the gradient operator with partial derivatives with respect to D_x

[3] *Karush-Kuhn-Tucker* conditions.

and D_y. Now, substituting ρ_1 by $\theta\rho_1$ and $\vec{D}_1$ by $\theta\vec{D}_1$,

$$\begin{aligned} \nabla_{\vec{D}} L(\theta\vec{D}_1, \nu_\theta^*)|_{\nu_\theta^* = \theta^{(p-1)}\nu_1^*} &= \theta^p \nabla_{\vec{D}} L(\vec{D}_1, \nu_1^*) \\ &= 0, \end{aligned}$$

and

$$\begin{aligned} \nabla \cdot \big(\theta\vec{D}_1(x,y)\big) - \theta\rho_1(x,y) &= \theta\big(\nabla \cdot \vec{D}_1(x,y) - \rho_1(x,y)\big) \\ &= 0 \end{aligned}$$

This can be easily verified using (4.1) and the fact that, for scalar θ, $\nabla \cdot \big(\theta\vec{D}(x,y)\big) = \theta\nabla \cdot \vec{D}(x,y)$. Therefore, $\theta\vec{D}_1(x,y)$ is the optimal solution for the *p-norm* problem (2.6) with load density function $\theta\rho_1(x,y)$. □

From now on, we assume $\vec{D}(x,y) = \theta\vec{D}_1(x,y)$ for a given initial flow field $\vec{D}_1$ and scaling factor $\theta \in \mathbb{R}^+$. With the above introduction, a formal definition of implementability can be stated as follows.

Definition 1: Let $\theta \in \mathbb{R}^+$ denote a positive scaling factor of $\vec{D}(x,y)$. Also, let $n(x,y;\theta)$ denote the density of nodes within the network, where $n(x,y;\theta) \to \infty$ as $\theta \to \infty$, $\forall (x,y) \in A$.

Information flow $\vec{D}(x,y)$ is implementable by a density of $n(x,y;\theta)$ nodes if there exists:

(a) transmission radius function $r_t(x,y;\theta)$ that goes to zero as $\theta \to \infty$, and

(b) increasing family of flow streamlines $\{f_i^\theta, i = 1, \cdots, n_s^\theta(A)\}$ of $\vec{D}$, and increasing family of streamline regions $\{h_i^\theta, i = 1, \cdots, n_s^\theta(A)\}$ associated with $\{f_i^\theta\}$,

such that w.h.p as $\theta \to \infty$

(i) $(n(x,y;\theta), r_t(x,y;\theta))$ topologically implement the flow streamlines $\{f_i^\theta\}$; i.e., without considering the possible interference due to simultaneous transmissions of nodes, connected paths can be formed to follow the flow streamlines $\{f_i^\theta\}$ within the margins of their associated regions $\{h_i^\theta\}$ by clusters of overlapping discs of radius $r_t(x,y;\theta)$ placed at nodes of density $n(x,y;\theta)$.

(ii) Multiple access schemes exist such that the topological implementation of the flow streamlines are sufficient to carry all of the traffic of $|\vec{D}|$.

Remark 1: As mentioned earlier, if the streamline seeding process which constructs the set of flow streamlines $\{f_i^\theta\}$ is such that it provides local regularity, then the required density of nodes is minimized. A seeding process provides local regularity if as $\theta \to \infty$, streamlines passing through any area element (with approximately uniform $|\vec{D}|$) eventually get evenly spaced for θ large enough.

4.2.1 Regular Streamline Seeding Process

The following seeding process can be performed in order to choose streamline seeds along the boundary of the distributed source such that the corresponding set of streamlines are locally regular as $\theta \to \infty$. For each value of the scaling factor θ, the flow seeds can be chosen by starting from an arbitrary point (x_1, y_1) on ∂D_s and placing the rest of the seeds on the boundary such that the line integral of $|\vec{D}|$ along ∂D_s between consecutive seeds is equal to the traffic to be relayed within each

streamline region. Let l be the parametric representation of ∂D_s. Then,

$$\int_{\substack{\text{consecutive}\\ \text{flow seeds}}} |\vec{D}| \mathrm{d}l \leq \gamma C. \tag{4.2}$$

The inequality in (4.2) is to take care of situations where $\frac{w_0}{\gamma C}$ is not an integer; hence, $n_s^\theta(A) = \lceil \frac{w_0}{\gamma C} \rceil = \frac{w_0}{\gamma C - \epsilon_\theta}$, where $\epsilon_\theta > 0$ is the smallest real value that makes the total number of streamlines be an integer value. Note that $\epsilon_\theta = o(1)$.

Due to smoothness of $|\vec{D}(x, y)|$, as θ increases, flow seeds get evenly spaced along each small segment of l. This is because when $|\vec{D}|$ changes smoothly along the boundary of the distributed source, it can be assumed to be approximately constant along small segments of l, hence (using (4.2)) as $\theta \to \infty$, $\Delta l = \frac{\gamma C}{|\vec{D}|}$, where Δl is the distance between flow seeds (for each small segment) on the boundary of the source with uniform $|\vec{D}|$. Hence, streamlines integrated from these flow seeds will be locally regular.

Remark 2: Let $\{f_i^\theta\}_r$ denote a set of streamlines selected using the regular seeding process, and $\{h_i^\theta\}_r$ be its associated set of streamline regions constructed by bisecting the area between consecutive streamlines, as described earlier. Then as $\theta \to \infty$, the width of streamline regions decreases proportional to θ^{-1} across any cross section of the network perpendicular to the flow field.

Remark 3: Consider a set of locally regular streamlines $\{f_i^\theta\}_r$ and its associated set of regions $\{h_i^\theta\}_r$, and for each i, let $g_i^\theta(t)$ denote the stochastic piecewise linear route inside streamline region h_i^θ with the same parametrization as for the flow streamlines. Then as $\theta \to \infty$, the set of piecewise linear routes $\{g_i^\theta\}_r$ converges

to the set of flow streamlines $\{f_i^\theta\}_r$ uniformly; i.e., $\lim_{\theta\to\infty} \max_i |f_i^\theta - g_i^\theta|_u \to 0$, where $|f_i^\theta - g_i^\theta|_u$ denotes the uniform distance (also called the supremum distance) between f_i^θ and g_i^θ which is defined as the maximum distance (greatest possible vertical distance) between the two functions from their initial starting points on the distributed source to the destination [65]. This is because using Remark 2, the width of streamline regions decrease proportional to θ^{-1} at any cross section of the network; hence, $\max_i \max_t\{\text{width } h_i^\theta\}$ shrinks to zero with the same proportion.

It is important to mention that although information flow is defined everywhere inside the network (including inside the distributed source), the implementability analysis (in the sense described in Definition 1) must be confined to the region between the distributed source and destination where the flow field is incompressible[4]. This is because in an incompressible field, assuming that every flow streamline is drawn continuously with no lines terminating at any point between the source and the sink, the magnitude $|\vec{D}|$ at any point is directly proportional to the number of streamlines crossing unit perpendicular line there [17]. This is further discussed in the sequel.

After describing the seeding process which constructs an increasing set of streamlines $\{f_i^\theta\}_r$, "suitable" transmission radius function $r_t(x, y; \theta)$ must be determined such that the rest of the conditions in Definition 1 are satisfied. In order to specify $r_t(x, y; \theta)$ at each point in the network and determine its relation with $|\vec{D}|$, the following steps are performed which will be described in detail subsequently:

- Perform a boundary-fitted flow-based gridding which results in a curvilinear

[4]divergenceless ($\nabla \cdot \vec{D} = 0$)

coordinate system and divides the network region into curvilinear grids with approximately uniform information flow inside each grid.

- Study the implementability problem inside each curvilinear grid.

- Extend the results to the network geometry.

Each of these steps will be described in detail in the subsequent sections.

4.3 Boundary-Fitted Flow-Based Gridding

The required density of nodes is a quantity which must be specified locally. Hence, the network region must be partitioned into smaller area grids over which the magnitude of information flow is approximately uniform. Granularity of grids is expected to decrease as they get closer to the sink.

The gridding step must be performed such that the implementability analysis along the boundaries becomes easier. Hence, grids should adapt to the features of information flow, i.e., the curvature of flow streamlines. This can be viewed as a curvilinear coordinate system for the network. Furthermore, since the information flow vector field satisfies the Neumann boundary condition (2.3), flow-based gridding of the network results in generation of boundary-fitted coordinates.

4.3.1 Existence of a Curvilinear Coordinate System

In this part, we discuss the existence of a boundary-fitted flow-based coordinate system for a network geometry with a given flow field[5]. In what follows, we show

[5]The following discussion is taken from [26].

that the existence of such coordinate system can be proved for flow fields which are ideal flows; i.e., flow fields that have zero divergence and zero curl. We use complex analytic functions to show the existence of such coordinate system and derive its properties. Specifically, the following theorems (stated without proof from [26]) are used to introduce a curvilinear coordinate system using complex analytic functions.

Consider steady state flow field $\vec{v}(x, y) = (u(x, y), w(x, y))$ at the point $(x, y) \in \Omega$. Here $\Omega \subset \mathbb{R}^2$ is the domain in which the flow field is defined.

Theorem 4.1: The flow vector field $\vec{v} = (u(x, y), w(x, y))$ induces an ideal flow if and only if $f(z) = u(x, y) - iw(x, y)$ is a complex analytic function of $z = x + iy$.

Hence, the components $u(x, y)$ and $-w(x, y)$ of an ideal flow field are harmonic conjugates. The corresponding complex function $f(z)$ is known as the *complex velocity* of the flow field.

Now, suppose that $f(z)$ admits a complex anti-derivative, i.e., a complex analytic function $\chi(z) = \phi(x, y) + i\psi(x, y)$ that satisfies $\frac{\mathrm{d}\chi}{\mathrm{d}z} = f(z)$. Then,

$$\frac{\mathrm{d}\chi}{\mathrm{d}z} = \frac{\partial\phi}{\partial x} - i\frac{\partial\phi}{\partial y} = u - iw \tag{4.3}$$

Therefore, $\nabla\phi = \vec{v}$. For this reason, the anti-derivative $\chi(z)$ is known as the complex potential function for the given flow field. Furthermore, $\phi(x, y)$ and $\psi(x, y)$ are referred to as the potential function and the stream function of the flow field,

respectively. Following the Cauchy-Riemann equations:

$$\begin{aligned} \frac{\partial \phi}{\partial x} &= \frac{\partial \psi}{\partial y} = u \\ \frac{\partial \phi}{\partial y} &= -\frac{\partial \psi}{\partial x} = w \end{aligned} \tag{4.4}$$

The level curves of the potential function, $\{\phi(x, y) = a\}$, where $a \in \mathbb{R}$ is fixed, are known as equipotential lines. The flow vector $\vec{v}$ points in the normal direction to the equipotential lines. On the other hand, as stated above, $\vec{v}$ is tangent to the level curves $\{\psi(x, y) = d\}$, $d \in \mathbb{R}$, of its harmonic conjugate stream function. But $\vec{v}$ is the flow field, and so tangent to the streamlines followed by the flow. Thus, these two systems of curves must coincide, and the level curves of the stream function are the streamlines of the flow.

Summarizing, for an ideal flow field, the equipotential lines $\{\phi = a\}$ and streamlines $\{\psi = d\}$ form mutually orthogonal systems of level curves. The flow field $\vec{v} = \nabla\phi$ is tangent to the streamlines and normal to the equipotential lines, whereas the gradient of the stream function, $\nabla\psi$, is tangent to the equipotential lines and normal to the streamlines.

The following theorem states the condition under which a unique anti-derivative function exists.

Theorem 4.2: Let $f(z) = \frac{\mathrm{d}\chi(z)}{\mathrm{d}z}$, where $\chi(z)$ is a single-valued complex function for $z \in \Omega$. If $c \subset \Omega$ is any closed curve, then $\oint_c f(z)\mathrm{d}z = 0$. Conversely, if this condition holds for all closed curves $c \subset \Omega$ contained in the domain of definition of $f(z)$, then f admits a single-valued complex anti-derivative $\chi(z)$ with $\frac{\mathrm{d}\chi(z)}{\mathrm{d}z} = f(z)$.

Based on the above discussion, there exists a flow-based coordinate system for the solution of the 2-*norm* flow problem (2.5) which, as shown in [1, 2], is irrotational (has zero curl) and incompressible (has zero divergence) in the region between the distributed source and destination. The properties of this coordinate system are studied next.

4.3.2 Properties of the Curvilinear Coordinate System

Following the aforementioned steps, the set of potential and stream functions of the ideal flow field $\vec{D}_1 = (D_{1,x}(x,y), D_{1,y}(x,y))$ can be represented by the following nonlinear transformation:

$$\begin{aligned} \mathbf{g} : A &\rightarrow \Phi \\ (x,y) &\mapsto (\phi(x,y), \psi(x,y)) \end{aligned} \tag{4.5}$$

Coordinate transformations and the properties of mapping between two domains can be specified using the Jacobian matrix and its determinant. The Jacobian matrix $\mathcal{J}$ represents local linear approximation to the change of coordinates between the two domains, and its determinant (referred to as the Jacobian J) is an area-change factor

from each element in the A-domain to the corresponding element in Φ-domain:

$$\begin{aligned} \mathcal{J} &= \begin{pmatrix} D_{1,x} & D_{1,y} \\ -D_{1,y} & D_{1,x} \end{pmatrix} \\ &= |\vec{D}_1| \begin{pmatrix} \frac{D_{1,x}}{|\vec{D}_1|} & \frac{D_{1,y}}{|\vec{D}_1|} \\ \frac{-D_{1,y}}{|\vec{D}_1|} & \frac{D_{1,x}}{|\vec{D}_1|} \end{pmatrix} \end{aligned} \tag{4.6}$$

It is important to note that the implementability analysis is performed in parts of the network where $|\vec{D}_1| \neq 0$, therefore $J \neq 0$. Now, using the inverse function theorem, the Jacobian matrix of the inverse transformation (from the Φ-domain to A) is equal to the inverse of the Jacobian matrix (4.6). Hence, the Jacobian matrix of the transformation from the Φ-domain to A is equal to

$$\mathcal{J}^{-1} = |\vec{D}_1|^{-1} \begin{pmatrix} \frac{D_{1,x}}{|\vec{D}_1|} & -\frac{D_{1,y}}{|\vec{D}_1|} \\ \frac{D_{1,y}}{|\vec{D}_1|} & \frac{D_{1,x}}{|\vec{D}_1|} \end{pmatrix} \tag{4.7}$$

The inverse transformation ($\mathbf{g}^{-1}$) describes how the network region A (which is a subspace of the Cartesian plane) is partitioned into curvilinear grids corresponding to equal partitioning of the ϕ and ψ axes in the Φ-domain. Note that the matrix in the right hand side of (4.7) is a rotation matrix. Hence, the transformation is conformal; i.e., the Jacobian matrix is a product of a rotation and scaling at all points. Such a map looks like a similarity transformation in small regions, even though it may significantly distort large shapes. Therefore, the grids of this curvilinear coordinate system can be approximated by square grids at each point in the

region between the distributed source and destination.

The flow-based gridding process in shown in Fig. 4.2, where solid curves represent flow streamlines of a given ideal flow within a subregion of the network and the curvilinear grid specified by dashed lines is the result of flow-based gridding. As shown in the figure, curvilinear lines derived from constant ψ in the Φ-domain are tangent to flow streamlines, and curvilinear lines derived from constant ϕ are perpendicular to the direction of flow of information.

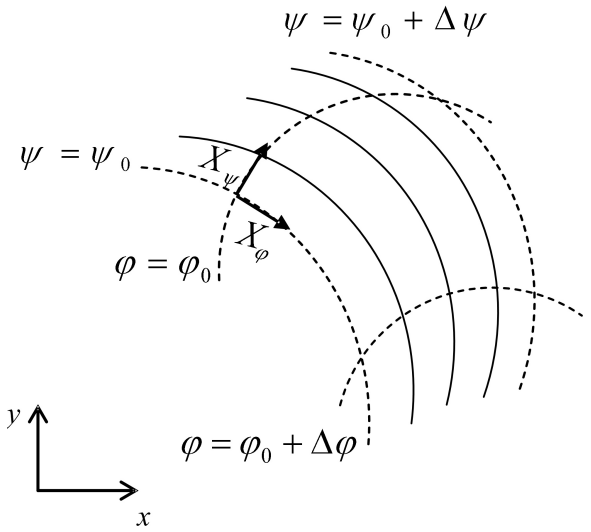

Figure 4.2: Flow-based gridding and curvilinear coordinates.

At the end, it is worth to mention that various numerical techniques for structured flow-based gridding have been proposed both within Cartesian and curvilinear grid frameworks [21–23]. These techniques are based on the use of streamlines computed from a single-phase flow problem. Also, a Jacobian-based elliptic grid generation technique is presented in [18]. This method, referred to as vector-field adaptive method or VFA, uses the idea of alignment with a given vector field indirectly via control of the inverse Jacobian matrix of the transformation.

4.4 Implementability Analysis Inside a Square Grid

In the previous section, we concluded that the network region can be partitioned into smaller approximately square grids which are tangent to the equipotential lines and flow streamlines of $\vec{D}_1$. Note that the size of these square grids varies throughout the network proportional to $|\vec{D}_1|^{-1}$. This is because, based on (4.7), the Jacobian of the mapping $\mathbf{g}^{-1}$ (from the Φ-domain to A) is equal to $|\vec{D}_1|^{-1}$ at every point in the network.

In this section, we study the implementability of the information flow inside a square grid as the scaling factor θ goes to infinity.

As the scaling factor θ increases, $|\vec{D}|$ scales linearly throughout the network and more flow streamlines are required to forward the traffic to the destination. Recall that the level curves of the curvilinear coordinate system are tangent to the equipotential lines and flow streamlines of $\vec{D}_1$; hence, flow streamlines passing through each grid are parallel to the sides of the grid.

Consider the unit square U_2 in the Φ-domain shown in Fig. 4.3 with uniform information flow $\vec{D}^{(l)} = \vec{D}(\phi, \psi)$ and flow streamlines parallel to the sides of the square. N sensors are distributed uniformly at random throughout the square and relay traffic to their downstream with equal transmission capacity of C bps, over a common wireless channel; hence, the total number of streamlines required to carry all the traffic within the square is $n_s(U_2) = O(\frac{|\vec{D}^{(l)}|}{C}) = O(|\vec{D}^{(l)}|)$.

Due to local regularity of the seeding process, streamlines are evenly spaced within the unit square. Hence, performing the bisection method, streamline regions

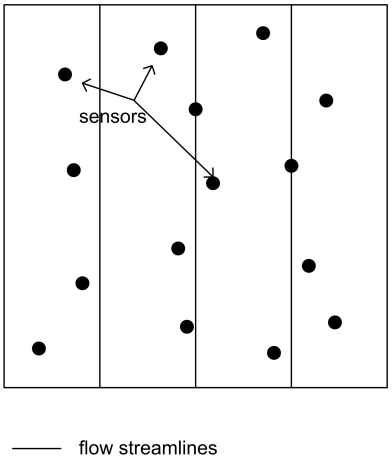

Figure 4.3: Unit square with uniform information flow and parallel streamlines.

are a set of $n_s(U_2)$ strips of equal width W_s, as shown in Fig. 4.4.

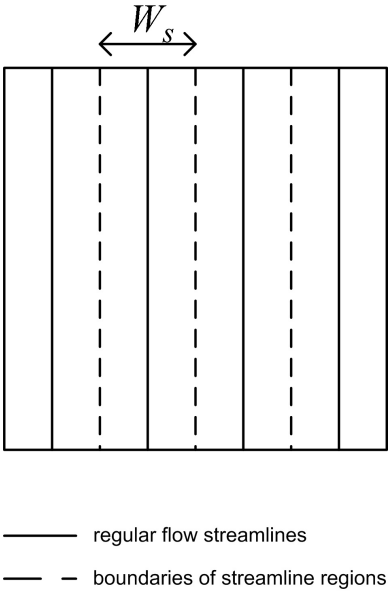

Figure 4.4: Unit square divided into $n_s(U_2)$ strips of width W_s.

In what follows, considering a Boolean model for communication which does not account for interference, it is shown that a quadratic relation between magnitude of information flow and density of nodes is not sufficient to follow flow streamlines resulting from discretizing the information flow. Hence, we conclude that a quadratic relation cannot guarantee implementability of information flow w.h.p under any

realistic communication model which accounts for interference from simultaneous transmissions. This is proved for the case where the set of streamlines are locally regular (evenly spaced). However, as explained in Remark 1, the locally regular case requires minimum node density for implementability. Thus, a quadratic relation cannot guarantee implementability regardless of whether or not the set of streamlines are locally regular.

Next, a sufficient bound for density of nodes is suggested and its sufficiency is shown under both communication models.

4.4.1 Topological Implementability Under a Quadratic Relation

Consider a bidirectional Boolean model for communication where nodes are connected to each other only if their distance is less than a specified transmission radius r_t. This link model represents wireless communication with signals diffusing isotropically with a certain signal attenuation. Let $p_t = p(r = 0)$ denote the signal power at the transmitter node and p_r denote the received power at a distance r from the transmitter. The received power falls off as $p_r \propto r^{-\alpha} p_t$, where α is the path loss exponent. The wireless transmission radius r_t can then be mapped to the equivalent transmission power p_t using a threshold Γ for receiver sensitivity; i.e., assuming that a node can receive properly if $p_r \geq \Gamma$. Obviously, this model does not account for the interference caused by possible simultaneous transmissions.

Let $G(N, r_t(N))$ be the communication graph formed by N nodes distributed uniformly at random in the unit square of Fig. 4.3, where $r_t(N)$ denotes the trans-

mission radius of each node. Let $X^{(l)}$ represent the location of nodes inside the unit square. Using the Boolean model, nodes $X_i^{(l)}$ and $X_j^{(l)}$ are connected if $|X_i^{(l)} - X_j^{(l)}| \leq r_t(N)$. Assuming all nodes use the same transmission radius for communication within the unit square, a well-studied problem is identifying the minimum radius (also called critical transmission radius r_c) such that the resulting communication graph is connected. A communication graph G is connected if and only if there exists at least one path connecting any pair of nodes in the network, and otherwise it is disconnected. As shown in [12], disconnectedness manifests itself by presence of isolated nodes. Isolated nodes cannot find any other nodes within their transmission radius. Lemma 4.2 investigates the minimum value of r_t such that $G(N, r_t(N))$ is connected w.h.p as $N \to \infty$.

As mentioned in Definition 1, the flow field is topologically implementable if, without considering possible interference due to simultaneous transmissions of nodes, connected paths can be formed to follow streamlines within the margins of their associated regions. Based on this definition, topological implementability of flow field inside the unit square is equivalent to existence of piecewise linear routes connecting the top to the bottom of the square within each region.

Connectivity of the communication graph $G(N, r_t(N))$ is not sufficient for topological implementability of the flow field $\vec{D}^{(l)}$, but as Lemma 4.3 states, it is a necessary condition for the flow field to be implementable.

In the following, we use the results from network connectivity and critical transmission radius in dense networks to prove that $N = O(|\vec{D}^{(l)}|^2)$ nodes is not sufficient to follow flow streamlines under the Boolean model. This shows that a

quadratic relation between number of sensor nodes and magnitude of information flow does not guarantee implementability of information flow.

Lemma 4.2: In order to ensure connectivity of $G(N, r_t(N))$ w.h.p, r_t must be chosen to be equal to or greater than the critical transmission radius

$$r_c = \sqrt{\frac{\log N + \eta(N)}{\pi N}}, \tag{4.8}$$

where $\eta(N)$ is an arbitrary function such that $\eta(N) \to \infty$ as $N \to \infty$.

Proof. See [24], Corollary 4.1.2. □

Substituting N by $O(|\vec{D}^{(l)}|^2)$ in equation (4.8) results in $r_c(|\vec{D}^{(l)}|) = \Omega(|\vec{D}^{(l)}|^{-1}\sqrt{\log|\vec{D}^{(l)}|})$. On the other hand, since implemented paths must not intersect with each other, the transmission radius r_t cannot be chosen to be greater than $O(W_s)$[6]. Furthermore, when adding interference to the model, if the order of transmission radius r_t is greater than W_s, transmission along a path will introduce interference to infinitely many other paths as $|\vec{D}^{(l)}| \to \infty$ and will significantly reduce the throughput of the network. Therefore, r_t must be chosen to be $O(W_s) = O(|\vec{D}^{(l)}|^{-1})$. Hence, $r_t < r_c$ as $|\vec{D}^{(l)}| \to \infty$. Considering the relation between transmission power and transmission radius, and using the same argument as above, transmission power of sensor nodes must also be $O(|\vec{D}^{(l)}|^{-\alpha})$ to reduce the amount of interference on simultaneous transmissions in neighboring implementation regions.

[6]Having a non-intersecting set of implemented paths can be guaranteed by assigning different frequency sub-channels to nodes residing in neighboring streamline regions. The required number of frequency sub-channels grow to infinity if $r_t > O(W_s)$ which significantly reduces the throughput.

Choosing $r_t < r_c$ results in a disconnected network; although we are not concerned with having a connected network in this work, but as stated earlier, disconnectedness manifests itself by presence of isolated nodes. Lemma 4.3 shows how the presence of isolated nodes affects topological implementability of flow streamlines.

Lemma 4.3: The set of flow streamlines inside the unit square cannot be topologically implementable if the pair (N, r_t) is chosen such that the network has isolated nodes w.h.p.

Proof. Throughout this argument, we assume that N nodes are distributed uniformly at random within the unit square. By the definition of topological implementability, if a set of flow streamlines is not implementable with (N, r_{t_1}), it cannot be implementable with any pair (N, r_{t_2}) such that $r_{t_2} < r_{t_1}$. Hence, without loss of generality, we will concentrate on cases where $r_t \geq W_s$.

Suppose $X_k^{(l)}$ is an isolated node in the network, and let d_{kf} denote its distance to the closest streamline. As mentioned before, the unit square is divided into $n_s(U_2)$ strips of width W_s; therefore, $0 \leq d_{kf} \leq \frac{W_s}{2}$.

Since $X_k^{(l)}$ is an isolated node, no other nodes exist in a region of distance r_t from $X_k^{(l)}$. This affects implementability of streamlines close to $X_k^{(l)}$, specifically the one within the same strip as $X_k^{(l)}$. For this streamline to get topologically implemented, there must exist at least one node inside the shaded area S_d shown in Fig. 4.5. Let $r_t = W_s$, and consider the largest S_d which corresponds to $d_{kf} = \frac{W_s}{2}$. Choosing a smaller d_{kf} can only decrease the probability of implementability.

$S_d|_{d_{kf}=\frac{W_s}{2}} = (\frac{\sqrt{3}}{4} - \frac{\pi}{12})W_s^2 = O(|\vec{D}^{(l)}|^{-2})$, and

$$\begin{aligned} P\{\text{the streamline not implementable}\} &\geq \\ P\{\text{there exists no node inside } S_d\} &= (1-S_d)^{N-1} \\ &\geq \exp(-\frac{(N-1)S_d}{1-S_d}) \end{aligned}$$

We have used Lemma 3.3 in the last inequality. Substituting N by $O(|\vec{D}^{(l)}|^2)$, and S_d by $O(|\vec{D}^{(l)}|^{-2})$, and taking the limit as $|\vec{D}^{(l)}| \to \infty$,

$$\lim_{|\vec{D}^{(l)}|\to\infty} P\{\text{the streamline not implementable}\} \geq \lim_{|\vec{D}^{(l)}|\to\infty} \exp(-NS_d) > 0$$

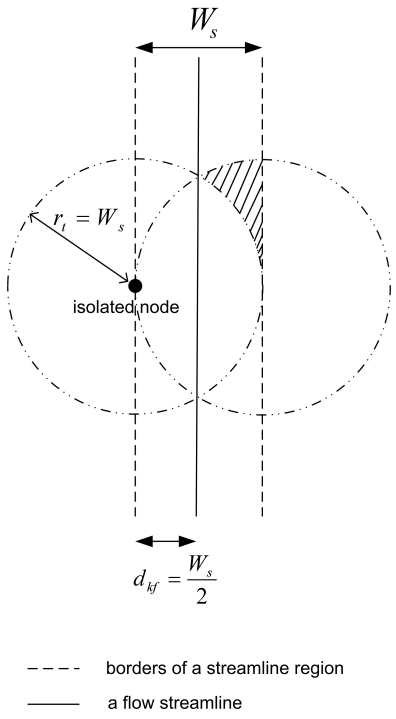

Figure 4.5: An isolated node affecting topological implementability of a flow streamline.

The above inequality states that the probability that the closest streamline to

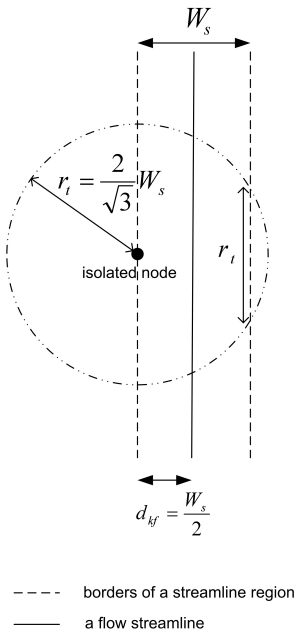

Figure 4.6: The area $S_d|_{d_{kf}=\frac{W_s}{2}} = 0$ for $r_t \geq \frac{2}{\sqrt{3}} W_s$.

$X_k^{(l)}$ is not topologically implementable is strictly positive. The same analysis can be done for $r_t > W_s$ resulting in a positive probability of the flow streamline not being implementable. Fig. 4.6 shows the scenario where $S_d|_{d_{kf}=\frac{W_s}{2}} = 0$ for $r_t = \frac{2}{\sqrt{3}} W_s$.

Note that this lemma is based on the assumption that the network has isolated nodes. Therefore, the transmission radius r_t cannot grow unconditionally and that it must be less than the critical transmission radius $r_c(N)$ for connectivity. □

Theorem 4.3: Information flow field $\vec{D}^{(l)}$ inside the unit square is not implementable with $N = O(|\vec{D}^{(l)}|^2)$ nodes distributed uniformly at random throughout the square.

Proof. Lemma 4.3, together with the fact that $r_t < r_c(|\vec{D}^{(l)}|)$ for $N = O(|\vec{D}^{(l)}|^2)$ proves that a quadratic relation between the total number of nodes and the traffic to be relayed does not guarantee existence of piecewise linear routes inside each

streamline region. Hence, $\vec{D}^{(l)}$ is not implementable with $N = O(|\vec{D}^{(l)}|^2)$ nodes distributed uniformly at random throughout the square. □

4.4.2 A Sufficient Order of Nodes for Implementability

The objective of this part is to find a sufficient bound on density of nodes with which flow streamlines are implementable. We show that a given information flow $\vec{D}^{(l)}$ in the unit square is implementable with $N = O(|\vec{D}^{(l)}|^2 \log |\vec{D}^{(l)}|)$ nodes distributed uniformly at random. The sufficiency of the bound is shown by applying feasible scheduling schemes under both the Protocol and the Physical Model. The proposed schemes follow the lines of thought in [25] and [7], and are briefly described here. A more detailed description of the methods are presented in Appendix B.

The main idea of the scheduling scheme is to divide time and frequency domains into smaller slots such that transmissions at each time slot and frequency sub-channel abide by either of the communication models.

Tessellate [7] the unit square into smaller square cells of length s similar to what is shown in Fig. 4.7. This divides the unit square into $\frac{1}{s^2}$ cells of equal size. Let $C_{a,b}$ denote a cell with coordinates $a, b = 1, \cdots, \frac{1}{s}$ starting from the bottom left, and let M be a fixed positive integer (to be determined later). Divide cells into M^2 groups $\{GC_i, i = 1, \cdots, M^2\}$ such that $C_{a,b}$ and $C_{a',b'}$ belong to the same group if and only if $a \equiv a' \pmod{M}$, and $b \equiv b' \pmod{M}$. Furthermore assume time is slotted, and each time frame has M^2 time slots. At each time slot $m = 1, \cdots, M^2$ only nodes within the mth group GC_m can communicate with their neighboring cells.

[7] Partition of an area into small units or subareas.

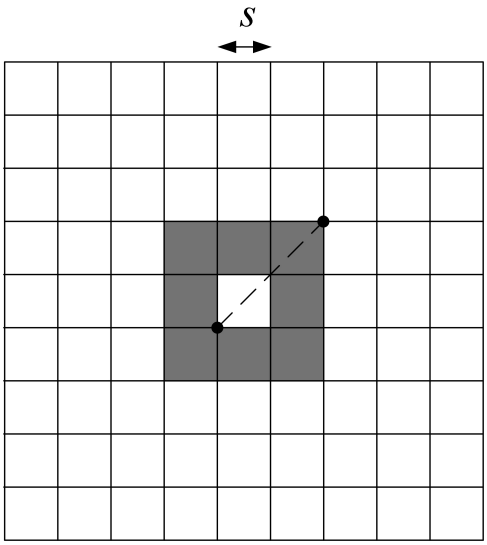

Figure 4.7: Tessellation of the unit square into cells of length s.

To ensure that the implemented paths do not intersect with each other, the length of each cell s is chosen to be $O(W_s)$, and the frequency channel is divided into $\kappa \geq 2$ sub-channels of equal capacity $\{C_i = \frac{C}{\kappa}, i = 1, \cdots, \kappa\}$. We use two sub-channels in the rest of this work; however as shown in the sequel, the linear relation between the total channel capacity C and each sub-channel's capacity C_i is sufficient to derive the bounds on N.

In order to guarantee that flow streamlines can be followed by piecewise linear routes, N must be chosen such that w.h.p there exists at least one node inside each cell. Furthermore, transmission power and correspondingly transmission radius of nodes must be such that inter-cell communications are possible with finite M as $|\vec{D}^{(l)}| \to \infty$. Suitable choice for M under each communication model is derived in Appendix B.

Theorem 4.4: Information flow $\vec{D}^{(l)}$ inside the unit square is implementable with $N = O(|\vec{D}^{(l)}|^2 \log |\vec{D}^{(l)}|)$ nodes distributed uniformly at random throughout

the square using either the Protocol or Physical Model.

Proof. See Appendix B. The proof shows that a finite M (independent of θ) can be found under either communication model, and that w.h.p there exists at least one node inside each cell of length $s = O(W_s) = O(|\vec{D}^{(l)}|^{-1})$ to relay traffic to its neighboring cell within its associated time slot. □

4.5 Extending the Results to the Network Geometry

Note that so far the unit square example (which corresponds to a curvilinear grid inside network A) is studied which only considers the interference effects inside the square. While this is acceptable for the Protocol Model which describes the effects of interference locally and on a pairwise relation between nodes, it may not be acceptable for the Physical Model which takes into account the aggregate interference from all nodes in the network communicating at the same time slot. The following lemma states that a bounded version of the Physical Model can be used for any arbitrary node X_i within the network and that the total interference due to simultaneous transmissions of nodes outside interference region $IR(X_i) = O(1)$ can be ignored in the implementability analysis. Hence, the results derived from the unit square can be extended to the rest of the network.

Lemma 4.4: A bounded version of the Physical Model with interference region $IR = O(1)$ can be used in the implementability analysis when nodes are communicating based on a controlled access scheme with transmission power $p_t \sim |\vec{D}|^{-\alpha}$.

Proof. Note that the flow-based gridding of the network region A is performed using the initial flow field $\vec{D}_1(x,y)$ and independent of the scaling factor θ. Hence, as θ grows, the size of curvilinear grids remains unchanged. However, transmission power of nodes changes proportional to $|\vec{D}|^{-\alpha} = \theta^{-\alpha}|\vec{D}_1|^{-\alpha}$. Also, the width of streamline regions shrinks proportional to $|\vec{D}|^{-1}$ at any cross section of the network. Consider interference region of nodes to be circular regions with radius of $O(1)$ around each node. Let $d(x,y)$ denote the density of active cells at each time slot. With the proposed TDMA scheme, $d(x,y) = \frac{1}{s^2M^2}$, where $s(x,y) = O(|\vec{D}(x,y)|^{-1})$ refers to the length of the tessellating cells inside each square grid, and M refers to the parameter of the controlled access scheme. Now, the total amount of interference at an arbitrary node X_u due to simultaneous transmission of nodes outside $IR(X_u)$ can be upper bounded as follows:

$$\begin{aligned} I_{A\setminus IR(X_u)} &\leq \max_s\{\frac{1}{s(x,y)^2M^2}\} \cdot \max_{(x,y)\in A\setminus IR(X_u)}\{p_t(x,y)\} \cdot O(1) \\ &= \frac{|\vec{D}_{\max}|^2}{|\vec{D}_{\min}|^\alpha} \cdot O(1) \\ &= \Big(\frac{|\vec{D}_{\max}|}{|\vec{D}_{\min}|}\Big)^2 \frac{1}{|\vec{D}_{\min}|^{\alpha-2}} \cdot O(1) \end{aligned} \tag{4.9}$$

Note that as $\theta \to \infty$, $\frac{|\vec{D}_{\max}|}{|\vec{D}_{\min}|}$ remains constant due to linear scaling of $|\vec{D}|$, and bounded due to non-zero dimensions of the information sink. Also, based on Lemma 4.1, as $\theta \to \infty$, $|\vec{D}| \to \infty$ everywhere in the network with non-zero information flow. Hence, the second term in (4.9) goes to 0 as $\theta \to \infty$.

With a diminishing interference effect at an arbitrary node X_u due to trans-

missions outside $IR(X_u)$, a bounded version of Physical Model (as stated in (1.6)) can be used for the implementability analysis. □

Hence, a sufficient bound on total number of nodes required to route traffic along a given ideal flow vector field $\vec{D}(x, y)$ (scaling linearly to infinity) inside any subregion A_s of the network is found by calculating the following integral

$$\int_{A_s} |\vec{D}(x,y)|^2 \log |\vec{D}(x,y)| \mathrm{d}x\mathrm{d}y. \tag{4.10}$$

The following example further illustrates the different steps involved in the implementability analysis.

Example: Consider a circle centered at the origin with radius R, as shown in Fig. 4.8, and assume that uniform information flow enters the circular area toward the sink which is located at the center. In order to avoid numerical ambiguities, information sink is assumed to be a circle with non-zero radius r_d. However, for simplicity, it is plotted as a point sink in the figure.

Assuming that the distributed source is located outside the circular area,

$$\rho(x, y) = 0, \;\; r_d^2 < x^2 + y^2 < R^2, \tag{4.11}$$

and the flow field is incompressible and irrotational everywhere within the circle except at the sink.

Let θ denote the total amount of traffic entering the circle. Hence, $n_s^{\theta}(A) = O(\frac{\theta}{C})$ streamlines are required to carry all the traffic to the sink. Following the

discretization method discussed in Section 4.2.1, any circle around the sink with radius $r_s > r_d$ can be used as a seeding path. Since the information flow passing through the seeding path is uniform along the path, flow seeds are placed regularly on the seeding path and streamlines are integrated all the way to the boundary of the network.

Using basic properties of information flow, the flow field $\vec{D}$ can be expressed in polar coordinates as follows:

$$\vec{D}(r,\phi) = -\frac{\theta}{2\pi r}\vec{a}_r, \quad r_d < r < R$$
$$\phi \in [0, 2\pi),$$

where $\vec{a}_r = \vec{Dir}(r,\phi)$ is the unit vector along the r-coordinate.

It can be easily verified that the level curves of the polar coordinates (r,ϕ) are tangent to the equipotential lines and flow streamlines of $\vec{D}_1(r,\phi) = -\frac{1}{2\pi r}\vec{a}_r$. Hence, polar coordinates is used to partition the circular area into grids of size $r\mathrm{d}r\mathrm{d}\phi$ with approximately uniform information flow inside each grid.

Using the results of Section 4.4.2, the required density of nodes to follow flow streamlines inside the each grid is of $O(|\vec{D}|^2 \log |\vec{D}|)$. Therefore, as $\theta \to \infty$, the total number of nodes sufficient to carry all the traffic to the destination is equal to

$$\int_0^{2\pi}\int_{r_d}^{R} \frac{\theta^2}{4\pi^2 r^2} \log \frac{\theta}{2\pi r} r\mathrm{d}r\mathrm{d}\phi = \frac{1}{2\pi} \log(\frac{R}{r_d}) \cdot \theta^2 \log(\frac{\theta}{2\pi\sqrt{r_d R}}).$$

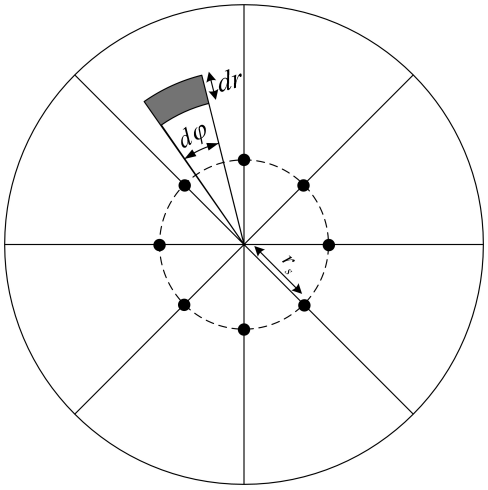

Figure 4.8: Streamline seeds are regularly placed on the circle with radius r_s from the sink.

4.6 Summary

In this chapter, we defined a new notion of connectivity, called implementability, which concerns the ability of sensor nodes to relay traffic along flow streamlines of a given information flow vector field $\vec{D}$. The concept of implementability is defined since the traditional definition of connectivity does not seem to be sufficient to satisfy the requirements of sensor networks, such as tight energy limitations and necessity of using lightweight protocol stacks.

In a network with a given information flow $\vec{D}$ (which is both incompressible and irrotational), we showed that a density of $n(x, y) = O(|\vec{D}(x, y)|^2)$ sensor nodes is not sufficient to implement the flow field, and that if the density increases to $n(x, y) = O(|\vec{D}(x, y)|^2 \log |\vec{D}(x, y)|)$ nodes, the flow field becomes implementable. The sufficiency of the latter is shown by proposing a controlled access scheduling scheme.

The excess amount of nodes required for implementability (compared to sim-

ply providing connectivity) can be exploited in cross-layer design and integration of protocol layers to make lightweight protocol stacks in order to meet specific requirements of dense sensor networks.

Chapter 5

Scalability Property of Dense Wireless Sensor Networks with Fading and Limited Buffer Capacity

5.1 Overview

In the first part of this chapter, we investigate the effects of fading on implementability of a given information flow vector field. We show that under a general model of fading presented in [7], the sufficient bound on density of nodes for following flux lines of an irrotational flow field need not be changed. The same methodology used in this part can be applied in [7] to provide a better lower bound on the throughput capacity of the network studied.

In the second part of this chapter, we deviate from using a slotted system and replace it with an asynchronous system with random transmission times. The use of a non-slotted protocol with random transmission times is justified later in Section 5.3.

In Chapter 4, we showed how level curves of the potential function and stream function of an irrotational flow field $\vec{D}_1(x, y)$ can be used to partition the network geometry into approximately square grids with uniform information flow inside each grid. We further showed that using this method, the implementability analysis of $\vec{D} = \theta\vec{D}_1$, $\theta \in \mathbb{R}^+$, is simplified to studying a square grid with uniform information

flow and with flow streamlines parallel to the sides of the square. We use the same technique in this chapter in studying the buffer scalability of sensor nodes forwarding traffic along flow streamlines of a given irrotational flow field with a linear scaling magnitude. As defined in [8], a protocol or a network architecture with nodes having limited buffer space is termed "buffer scalable" if the performance of the network does not degrade as its size grows to infinity.

Therefore, once again, we concentrate on a unit square with uniform flow field $\vec{D}^{(l)}$ and flow streamlines parallel to the sides of the square for performing buffer scalability analysis of networks routing along a given irrotational direction field. We show that the traffic flux $|\vec{D}^{(l)}|$ entering the square can be forwarded along the flow streamlines with $N = O(|\vec{D}^{(l)}|^2 \log |\vec{D}^{(l)}|)$ nodes, while the buffer space of sensor nodes need not grow as $|\vec{D}^{(l)}| \to \infty$. This result is particularly interesting for dense WSNs where nodes are assumed to have very limited resources.

Furthermore, we show that buffer scalability of the network is conserved under fading and that sensor nodes can forward traffic along flow streamlines with finite buffer spaces.

5.1.1 Related Work

Many works in the literature on wireless networks [7, 13, 45, 46] consider slotted systems with deterministic transmission times justified by the presence of a centralized scheduler. However, centralized algorithms have global synchronization overhead and are unlikely to be feasible in large ad-hoc networks.

There has also been an extensive amount of work [31, 49, 51] done in modeling wireless networks as queueing networks where nodes are modeled as queues with infinite buffer size. The approximation of infinite buffer space is made to simplify the analysis of such networks; however it is not realistic under the context of wireless networks.

On the other hand, analyzing large networks with finite buffers is difficult since no analytical solutions like the product-form of Jackson networks are available, and hence queueing approximations are used instead [52]. Most of these assumptions are based on Jackson's independence assumption which works well under low arrival rates and degrades rapidly as the rate increases [52]. For example, [48] analyzes the intensity of relayed traffic in a wireless mesh network using a M/M/1/K queueing model, and neglects the existing correlation between the traffic and queue occupancy of neighbor nodes. On the other hand, authors of [39] propose an analysis that captures the dependence between queue distribution of different nodes and achieves more accurate distributions for higher rates.

Authors of [55] evaluate the throughput of two different packet scheduling policies under uniform traffic assumption for the infinite and finite buffer cases in a hypercube. They remarked that small buffer sizes can achieve throughput close to that of the infinite buffer case. Similarly in the context of static wireless ad hoc networks, [8] focuses on how the maximum throughput in large wireless networks scales with finite buffers. The authors demonstrate that the network cannot operate at its capacity limit while maintaining a constant buffer space in each node. They further construct a scalable protocol that obtains just a slightly smaller throughput

with fixed buffers, capable of storing only a few packets. Finally from a mathematical perspective, [8] furthers our understanding of the difficult problem of analyzing large queueing networks with finite buffers.

5.1.2 Communication Model

In this chapter we concentrate on the Physical Model. Again, let X_i denote the location of a node as well as the node itself. Assuming that the channel bandwidth used for wireless communication is much less than the channel coherence bandwidth[1] B_{coh}, the channel is frequency non-selective or flat; that is, the fading is roughly equal across the entire signal bandwidth [41]. Under this assumption, the channel will only have a multiplicative effect on signals. Now considering path loss and fading effects and transmission power p_t, the received power from node X_i to node X_j is equal to $g_{ij}\frac{p_t}{|X_i - X_j|^\alpha}$, where $|\cdot|$ represents the Euclidean distance between two points in the Cartesian plane and α represents the loss factor. g_{ij} refers to the fading coefficient. In the absence of fading, $g_{ij} = 1$, $\forall i, j$. In the presence of fading, g_{ij} is a non-negative random variable which does not change with time. This is because we assume that sensor nodes are static and only one channel realization is observed over time. A more detailed discussion on fading channels is presented in Appendix A.

We follow the same assumptions used in [7] regarding the fading coefficients. In particular, we assume fading coefficients are independent and identically dis-

[1]Coherence bandwidth is the range of frequencies over which any two frequency components have a strong correlation.

tributed (i.i.d) and $g_{ij} = g_{ji}$. We also assume that fading coefficients have expectation $E[g_{ij}] = 1$ and exponentially decaying tails; i.e., letting $F^c(x)$ denote their complementary cumulative distribution function:

$$F^c(x) = P[g_{ij} > x] \leq \exp(-qx), \forall x > x_1, \tag{5.1}$$

for some real and positive parameters q and x_1[2]. Furthermore, we assume that there is a median $g_m > 0$ such that $P[g_{ij} \geq g_m] \geq \frac{1}{2}$. Although the assumptions above might look restrictive, they are satisfied by most distributions used to model fading [56].

With combined path loss and fading effects in a homogeneous network scenario where all nodes use same transmission power, the SINR between X_i and X_j is equal to

$$SINR = \frac{g_{ij} \frac{p_t}{|X_i - X_j|^\alpha}}{N_0 + \sum_{\substack{k \in T \\ k \neq i}} g_{kj} \frac{p_t}{|X_k - X_j|^\alpha}}, \tag{5.2}$$

where $\{X_k, k \in T\}$ is the set of nodes simultaneously transmitting over the same channel as X_i. As mentioned earlier, for a successful transmission between two nodes under the Physical Model

$$SINR \geq \Gamma \tag{5.3}$$

The value of Γ is fixed and is determined for each application based on the desired

[2]Relation (5.1) results in fading coefficients to have finite second moment; i.e., $E[g_{ij}^2] < \infty$

data rate, modulation scheme, etc.

5.2 Implementability of Information Flow Under Fading

The goal of this section is to analyze the effect of fading on implementability of information flow. As mentioned earlier, we follow the same assumptions made in [7] regarding the fading coefficients.

Consider a unit square as shown in Fig. 4.3 with uniform information flow $\vec{D}^{(l)}$ and flow streamlines parallel to the sides of the square. As discussed in Chapter 4, the region between the source and destination of a network with an ideal information flow vector field can be partitioned into smaller approximately square grids resembling the unit square shown in Fig. 4.3.

Once again, consider tessellating the unit square into smaller cells as described in Section 4.4.2. Under the no-fading scenario, the TDMA scheme outlined in Chapter 4 works based on choosing M large enough such that transmissions at each time slot are successful based on the Physical Model. Therefore, N is chosen such that w.h.p there exists at least one node inside each cell to forward traffic to its downstream or receive traffic from its upstream.

Under fading, similar to [7], we assume that when a node wants to transmit it will pick as the receiver any of the nodes in the neighboring cell whose link with the transmitter has a fading coefficient greater than or equal to g_m. This is done to reduce the complexity of choosing the next node because of the unbounded support of fading coefficients. Hence, N must be chosen large enough such that each node

in a cell can find w.h.p at least one node in its neighboring cell with which their mutual fading coefficient is greater than or equal to g_m.

Equation (5.2) states that (in the absence of fading) the amount of interference caused by simultaneous transmitters X_k decreases due to path loss effects as their distance from the receiver node X_j increases. However, fading coefficients are i.i.d and have unbounded support; hence, even nodes far away from the receiver might still cause a considerable amount of interference. Therefore, bounding the total interference is an important concern when exploring spatial diversity under fading.

We use Kolmogorov's Three-Series Theorem [47] to show that under fading, the total interference caused by simultaneous transmissions using the aforementioned TDMA scheme is bounded almost surely (a.s.); this theorem is stated as a lemma for Theorem 5.1.

Lemma 5.1: *(Kolmogorov's Three-Series Theorem)* Let $\mathcal{A} > 0$. Suppose $\{Z_i\}_{i=1}^{\infty}$ are independent random variables and set $Y_k = Z_k 1\{|Z_k| < \mathcal{A}\}$, $\forall k \geq 1$; then $\sum_{k=1}^{n} Z_k$ converges a.s. as $n \to \infty$ if and only if

(i) $\sum_{k=1}^{\infty} P[|Z_k| > \mathcal{A}] < \infty$

(ii) $\sum_{k=1}^{\infty} E[Y_k]$ converges to a finite limit

(iii) $\sum_{k=1}^{\infty} Var[Y_k] < \infty$

Proof. See [47], Theorem 2.5.4. □

Theorem 5.1: Information flow $\vec{D}^{(l)}$ inside the unit square is implementable with $N = O(|\vec{D}^{(l)}|^2 \log |\vec{D}^{(l)}|)$ nodes distributed uniformly at random throughout

the square, in the presence of fading.

Proof. The same TDMA scheme outlined in Chapter 4 can be used to show the sufficiency of $N = O(|\vec{D^{(l)}}|^2 \log |\vec{D^{(l)}}|)$ nodes in following flow streamlines within each streamline region under fading. In order to follow the same scheme, we need to show that

(I) All nodes can find w.h.p at least one node in their neighboring cells with which their fading coefficient is greater than or equal to g_m. This guarantees that intercell communication is possible and that nodes inside each cell can find other nodes in their neighboring cells to communicate with that satisfy the required condition for routing under fading. The proof of this part is very similar to the proof of part 1 of Theorem 2 in [7].

(II) The total interference $I(M)$ resulting from tessellating the unit square into M^2 groups of cells and using a TDMA scheme of M^2 slots per time frame is bounded a.s.: Let $X_i^{(l)}$ denote a node transmitting to node $X_j^{(l)}$, and let $\{X_k^{(l)}, k \in T\}$ denote all nodes transmitting in the same time slot and sub-channel as $X_i^{(l)}$. Cells that are simultaneously active with each other occupy different tiers, and can be categorized as described in Table B.1. In order to simplify the analysis, let us deviate from the previous notation of the fading coefficients and, only in the context of this proof, use g_{kv} to refer to the fading coefficient between the transmitter located in the kth active cell of tier v around $X_i^{(l)}$ and the receiver node $X_j^{(l)}$.

Now, the total interference $I(M)$, which is a function of M, can be upper

bounded as follows:

$$
\begin{aligned}
I(M) &\leq \sum_{v=1}^{\infty}\sum_{k=1}^{8v}\frac{g_{kv}p_t}{\big((vM-2)s\big)^{\alpha}} \\
&= \frac{p_t}{s^{\alpha}}\sum_{v=1}^{\infty}\frac{8v}{(vM-2)^{\alpha}}\frac{\sum_{k=1}^{8v}g_{kv}}{8v} \\
&= \frac{8p_t}{Ms^{\alpha}}\sum_{v=1}^{\infty}\Big(\frac{1}{(vM-2)^{\alpha-1}}+\frac{2}{(vM-2)^{\alpha}}\Big)\Xi_v \\
&\leq \frac{8p_t}{Ms^{\alpha}}\sum_{v=1}^{\infty}(v^{-\alpha+1}+2v^{-\alpha})\Xi_v,
\end{aligned}
\tag{5.4}
$$

where v refers to the tiers with cells that are in the same group as the cell of $X_i^{(l)}$, and k counts the number of cells at each tier that are simultaneously active with $X_i^{(l)}$. In the third line of (5.4), we have defined $\Xi_v = \frac{\sum_{k=1}^{8v}g_{kv}}{8v}$. Note that $\{\Xi_v\}_{v=1}^{\infty}$ are independent and non-negative random variables with $E[\Xi_v] = 1$ and $Var[\Xi_v] = \frac{\sigma_g^2}{8v}$, where σ_g^2 refers to the variance of the fading coefficients. Finally, the last inequality is derived using the fact that $vM-2 \geq v$, for M large enough.

In order to prove the boundedness of total interference we need to show that $\sum_{v=1}^{\infty} v^{-r}\Xi_v$ is bounded for $r > 1$, a.s. This can be verified using Lemma 5.1. Let $\zeta(r) = \sum_{v=1}^{\infty} v^{-r}$, and note that $\zeta(r) > 1$ and is strictly bounded for $r > 1$. Now, let $Z_v = v^{-r}\Xi_v$ and $\mathcal{A} > 1$, as defined in Lemma 5.1, and check if the necessary and sufficient conditions for convergence hold:

(i)

$$\begin{aligned}\sum_{v=1}^{\infty} P[Z_v > \mathcal{A}] &= \sum_{v=1}^{\infty} P[\Xi_v > \mathcal{A}v^r] \\ &\leq \frac{1}{\mathcal{A}} \sum_{v=1}^{\infty} v^{-r} \\ &= \frac{1}{\mathcal{A}} \zeta(r) < \infty\end{aligned}$$

The second line is derived using the Markov inequality.

(ii)

$$\begin{aligned}\sum_{v=1}^{\infty} E[Z_v 1\{Z_v < \mathcal{A}\}] &\leq \sum_{v=1}^{\infty} E[Z_v] \\ &= \sum_{v=1}^{\infty} v^{-r} = \zeta(r), \text{ for } r > 1\end{aligned}$$

Convergence of $\Big\{E[Z_i 1\{Z_i < \mathcal{A}\}]\Big\}_{i=1}^{\infty}$ can be verified by performing a comparison test with $\Big\{E[Z_i]\Big\}_{i=1}^{\infty}$.

(iii)

$$\begin{aligned}\sum_{v=1}^{\infty} Var[Y_v] \leq \quad \sum_{v=1}^{\infty} E[Y_v^2] \qquad &\leq \sum_{v=1}^{\infty} E[Z_v^2] \\ = \quad \sum_{v=1}^{\infty} v^{-2r}(\tfrac{\sigma_g^2}{8v} + 1) = \quad &\frac{\sigma_g^2}{8}\zeta(2r+1) + \zeta(2r)\end{aligned}$$

All three conditions hold; hence, the series converges and $I(M)$ is bounded a.s.

(III) There exists a finite M_{Phy}^f independent of θ (the scaling factor of $|\vec{D}^{(l)}|$) such

that transmissions at each time slot m are successful based on the Physical Model provided that $M \geq M^f_{Phy}$:

Let p_r denote the received power at a node. Since nodes communicate only with their neighboring cells,

$$p_r \geq \frac{g_m p_t}{(2\sqrt{2}s)^\alpha} \tag{5.5}$$

From relations (5.4) and (5.5), the total SINR ratio can be lower bounded by

$$SINR \geq \frac{\frac{g_m p_t}{(2\sqrt{2})^\alpha s^\alpha}}{N_0 + I(M)}$$

By choosing the right hand side of the relation above to be greater than or equal to Γ, the SINR ratio of each transmission is guaranteed to satisfy the Physical Model requirement. Hence, substituting $I(M) = a\frac{p_t}{Ms^\alpha}$, for some $a > 0$, and solving for M,

$$M \geq \frac{\Gamma a \frac{p_t}{s^\alpha}}{\frac{g_m p_t}{(2\sqrt{2})^\alpha s^\alpha} - \Gamma N_0} \tag{5.6}$$

As discussed in the previous chapter, $s = O(|\vec{D}^{(l)}|^{-1})$ and $p_t = O(|\vec{D}^{(l)}|^{-\alpha})$; hence, $\frac{p_t}{s^\alpha}$ converges to a constant as $|\vec{D}^{(l)}| \to \infty$. Also, for any given Γ, the transmission power p_t can be chosen such that the denominator in (5.6) is positive. Hence, M can be chosen to be large enough such that the lower bound on the SINR is met in each transmission.

This concludes the proof. □

Remark 1: Similar to Theorem 5.1, Lemma 5.1 can also be applied to [7] in which Toumpis and Goldsmith study the throughput capacity of a network of n immobile nodes, each with a destination node chosen at random. The devised scheme in [7] guarantees a per node communication rate under fading that (compared to the case with no fading) is not reduced by more than a logarithmic factor[3]. Particularly, using the Kolmogorov's Three-Series Theorem, one can show in [7] that the amount of interference and hence the total SINR under fading is proportional to the case with no fading. Therefore, the network can provide each node with a traffic rate of the same order in the absence or presence of fading.

For the sake of completeness and in order to be able to extend the results of the unit square to more general network geometries, we state a modified version of Lemma 4.4 to show that (even in the presence of fading) a bounded version of the Physical Model can be used for any arbitrary node X_i within the network and that the total interference due to simultaneous transmissions of nodes outside interference region $IR(X_i) = O(1)$ can be ignored in the implementability analysis. Hence, the results derived from the unit square can be extended to the rest of the network.

Lemma 5.2: A bounded version of the Physical Model with interference region $IR = O(1)$ can be used in the implementability analysis when nodes are communicating based on a controlled access scheme with transmission power $p_t \sim$

[3]Note that authors in [7] do not imply that the traffic carrying capacity of the network is reduced in the presence of fading. They rather specify lower bounds on the capacity, in terms of uniformly achievable rates of communication. In fact, the authors conjecture that the lower bound for the capacity in the presence of fading is as tight as the bound for the capacity in the non-fading case, up to a logarithmic factor [7]. However, they do not investigate this conjecture.

$|\vec{D}|^{-\alpha}$, in the presence of fading.

Proof. Consider interference region of nodes to be circular regions with constant radius r_0 around each node. Let $d(x, y)$ denote the density of active cells at each time slot. As shown in the proof of Lemma 4.4, $d(x, y) \sim |\vec{D}|^2$. Now, the total number of nodes outside the interference region of an arbitrary node X_u which are simultaneously transmitting data is equal to

$$N_{A\setminus IR(X_u)} = \int_{A\setminus IR(X_u)} d(x, y)\mathrm{d}x\mathrm{d}y$$

Based on the above relation and considering the fact that $d(x, y) \sim |\vec{D}(x, y)|^2$, $N_{A\setminus IR(X_u)} = \Theta(\theta^2)$, where θ is the scaling factor of the information flow vector field. Therefore, the total amount of interference at node X_u due to simultaneous transmission of nodes outside $IR(X_u)$ can be upper bounded as follows:

$$\begin{aligned} I_{A\setminus IR(X_u)} &\leq \sum_{k=1}^{N_{A\setminus IR(X_u)}} g_{ku} \frac{p_{t,k}}{|X_k - X_u|^\alpha} \\ &\leq \frac{\max_k\{p_{t,k}\} N_{A\setminus IR(X_u)}}{r_0^\alpha} \frac{\sum_{k=1}^{N_{A\setminus IR(X_u)}} g_{ku}}{N_{A\setminus IR(X_u)}} \end{aligned}$$

Now based on the Strong Law of Large Numbers (SLLN), as $\theta \to \infty$,

$$\frac{\sum_{k=1}^{N_{A\setminus IR(X_u)}} g_{ku}}{N_{A\setminus IR(X_u)}} \overset{a.s.}{\to} 1$$

Therefore,

$$\begin{aligned} I_{A\setminus IR(X_u)} &\leq \frac{\max_k\{p_{t,k}\}N_{A\setminus IR(X_u)}}{r_0^{\alpha}} \\ &= \theta^{-(\alpha-2)}O(1), \end{aligned}$$

which goes to 0 as $\theta \to \infty$. □

With a diminishing interference effect at an arbitrary node X_u due to transmissions outside $IR(X_u)$, a bounded version of the Physical Model can be used for the implementability analysis in the presence of fading.

5.3 Buffer Scalability of Sensor Nodes Routing Along Flow Flux Lines

In this section, we investigate the behavior of sensor nodes deployed uniformly at random within the unit square as $|\vec{D}^{(l)}|$ scales linearly to infinity while the buffer space of each sensor node remains constant. In other words, we investigate buffer scalability of the unit square network which is defined as the quality of a protocol or a network architecture such that the performance of the network does not degrade as its size grows[4], due to the limited buffer space in each node [8].

In this part we deviate from assuming a synchronous slotted system of communication and adopt an asynchronous system where transmissions at each time slot are *possible* under (5.3) with a random transmission time with finite mean. Asyn-

[4]Note that the area of dense networks is constant. In this chapter, network size refers to the number of sensor nodes which grows as the magnitude of information flow increases.

chronous operation and random transmission times can be justified as follows [8]:

- Centralized scheduling is unlikely to be feasible in dense WSNs. Hence, distributed scheduling might be used which results in asynchronous transmissions.

- The physical channel might be highly variable, and therefore, in certain time intervals no transmissions might be feasible due to transmission errors on the data-link layer.

- Possible collisions on the MAC layer might also contribute to such randomness.

In the asynchronous model, the traffic flux entering any small area element of the network with approximately uniform flow field $\vec{D}$ is modeled as a spatial Poisson process with intensity $|\vec{D}|\frac{\text{pps}}{\text{unit width}}$[5]. Similarly, when studying the unit square network, the traffic flux entering the square is assumed to be a Poisson process with intensity $|\vec{D}^{(l)}|\frac{\text{pps}}{\text{unit width}}$. To investigate buffer scalability, sensor nodes are assumed to have a finite buffer capable of storing b packets. Generally, packet size might need to be an increasing function of the number of nodes in a network in order to keep the payload size constant; however, since the location of data sink is assumed to be fixed in our work, data packets are assumed to have constant size of l_p bits.

5.3.1 Without Fading

Let us first consider the case where the wireless medium does not have fading effects; i.e., all fading coefficients are equal to 1. Since sensor nodes have finite buffer

[5]pps: packets per second

space, a "buffer coordination algorithm" as defined in [8] must be deployed in order to avoid unnecessary network performance degradation. The goal of such algorithm is the efficient use of buffer space in each cell. To motivate the necessity of deploying such an algorithm, consider the following scenario. Suppose a node requires to relay a packet to a node in its neighboring cell. To forward traffic toward the sink, the node can send its packet to any of the nodes in the neighboring cell. However, if the relay node is chosen without considering its buffer contents, an unnecessary packet loss can occur. A buffer coordination algorithm assists nodes in neighboring cells to forward packets to nodes that have available buffer space, when possible. Hence, packet loss occurs only if no node in a cell has available buffer space. The design of such an algorithm is beyond the scope of this work. However as mentioned in [8], it could be designed using a token-based approach under the First-Come-First-Served (FCFS) scheduling policy.

By deploying a buffer coordination algorithm, each cell can be modeled as a supernode with buffer size equal to the sum of the buffer spaces of nodes inside the cell. The service time of supernodes is assumed to be exponentially distributed with mean $\frac{1}{\mu} = \frac{\kappa l_p}{C}$ pps^{-1}, where κ refers to the number of frequency sub-channels used for data transmission. For simplicity, we assume that packets are served on a FCFS discipline.

The width of streamline regions is chosen such that the arrival rate λ of data packets (measured in pps) into each region is less than the transmission capacity $\frac{C}{\kappa l_p}$ pps . In order to simplify the analysis of buffer scalability, we assume that there is limited or no cross-traffic interference along information flow paths from the source

to the destination. This is reasonable since the wireless channel is divided into $\kappa \geq 2$ sub-channels such that no neighboring streamline regions share the same sub-channel. Using this assumption, streamline regions can be analyzed independently from each other.

Recall that the unit square is tessellated into square cells of size $s = O(|\vec{D}^{(l)}|^{-1})$. Hence, each streamline region can be modeled as a linear network of size $\varsigma = O(|\vec{D}^{(l)}|)$. Indexing supernodes inside a streamline region by $1, 2, \cdots, \varsigma$, data packets enter at supernode 1 according to a Poisson process of rate λ pps. Data packets are relayed between supernodes in the network. A packet transmitted by the ith supernode is received by the $(i+1)$th supernode. When it is relayed to the ςth supernode and is successfully transmitted, the packet reaches the bottom of the network.

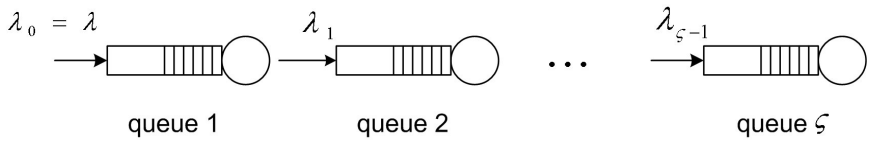

Figure 5.1: Linear network modeling relay of traffic inside each streamline region. Each queue represents a supernode (cell) and has buffer size b_s.

By modeling nodes inside each streamline region as a linear network, we can use the results from linear network analysis [8, 9] to investigate buffer scalability of sensor nodes inside the unit square.

Lemma 5.3: Consider k nodes in tandem where each node has a buffer space of size b'. Packets arrive to the first node according to a Poisson process of rate λ_0 and are relayed between nodes until they reach the kth node. Service times are assumed to be exponential and independent from the arrival process as well as

independent from each other. Let λ_k denote the rate at which packets leave the last node. In order to keep $\lambda_k = \Theta(1)$ as $k \to \infty$, $b' = O(\log k)$. Note that this is a necessary and sufficient condition.

Proof. See Section III of [8] for a complete proof. □

Remark 2: In a condition where the input and output throughputs (λ_0 and λ_k) are proportional asymptotically, the probability of an arbitrary packet being lost in the network is strictly bounded away from 1 as the network size increases.

Lemma 5.4: Consider tessellating the unit square into cells of size $s = O(|\vec{D}^{(l)}|^{-1})$, and distributing $N = k_1|\vec{D}^{(l)}|^2 \log|\vec{D}^{(l)}|$ nodes uniformly at random throughout the square. Let $N_{i,j}$ denote the number of nodes inside each cell $C_{i,j}$, $i, j = 1, \cdots, \frac{1}{s}$. For k_1 large enough, as $|\vec{D}^{(l)}| \to \infty$,

$$P[\frac{k_2}{3}\log|\vec{D}^{(l)}| \leq N_{i,j} \leq k_2 \log|\vec{D}^{(l)}|, \forall i, j = 1, \cdots, \frac{1}{s}] \to 1, \tag{5.7}$$

where k_2 is a constant proportional to k_1.

Proof. We use the following versions of Chernoff's bound to prove the lemma [53]: For a binomially distributed random variable X with parameters n (number of Bernoulli trials) and p (probability of success of each trial), and for any $\delta \in (0, 1]$,

$$P[X < (1-\delta)np] < \exp(-np\frac{\delta^2}{2}), \tag{5.8}$$

and for any $\delta > 0$,

$$P[X > (1+\delta)np] < [\frac{\exp(\delta)}{(1+\delta)^{(1+\delta)}}]^{np}. \tag{5.9}$$

Let $s = a|\vec{D}^{(l)}|^{-1}$ for some real $a > 0$. Using (5.8) with $\delta = \frac{1}{2}$, and considering the fact that $N_{i,j} \sim \text{Binom}(N, s^2)$:

$$\begin{aligned} P[N_{i,j} < \frac{k_1 a^2}{2} \log|\vec{D}^{(l)}|] &\leq \exp(-\frac{k_1 a^2}{8} \log|\vec{D}^{(l)}|) \\ &= |\vec{D}^{(l)}|^{-\frac{k_1 a^2}{8}} \end{aligned} \tag{5.10}$$

On the other hand, using (5.9):

$$\begin{aligned} P[N_{i,j} > \frac{3k_1 a^2}{2} \log|\vec{D}^{(l)}|] &\leq \exp(-\varepsilon k_1 a^2 \log|\vec{D}^{(l)}|) \\ &= |\vec{D}^{(l)}|^{-\varepsilon k_1 a^2}, \end{aligned} \tag{5.11}$$

where $\varepsilon = \frac{3}{2}\log\frac{3}{2} - \frac{1}{2}$. Now, letting $k_2 = \frac{3k_1 a^2}{2}$ and using the union bound, the result is concluded for $k_1 > \frac{2}{\varepsilon a^2}$. □

Theorem 5.2: As $|\vec{D}^{(l)}| \to \infty$, the unit square network is buffer scalable with $N = O(|\vec{D}^{(l)}|^2 \log|\vec{D}^{(l)}|)$ nodes deployed uniformly at random each having a buffer space of size $b = 1$.

Proof. In the unit square network, sensor nodes must be able to relay traffic from the top to the bottom with an end-to-end probability of packet loss which is strictly less than 1 and does not grow as $|\vec{D}^{(l)}| \to \infty$. Based on Lemma 5.3, a necessary and sufficient condition for each supernode to maintain such end-to-end performance in-

side streamline regions is to have a buffer space of size $b_s = O(\log \varsigma) = O(\log |\vec{D}^{(l)}|)$. Due to deployment of a buffer coordination algorithm, buffer space of each supernode is equal to the sum of buffer spaces of sensor nodes inside the cell of which it represents. Letting $b = 1$ for sensor nodes and using Lemma 5.4, we conclude the result. □

Based on Theorem 5.2, by using a buffer coordination algorithm nodes can have very limited buffer space when routing along information flow flux lines. This is particularly interesting for dense WSNs where nodes are desired to have very limited resources.

5.3.2 With Fading

As stated in Lemma 5.3, in order to have a constant throughput inside each streamline region, supernodes modeling each cell must have buffer space of size $b_s = O(\log |\vec{D}^{(l)}|)$. Without considering the fading effects, by using the result of Lemma 5.3, the number of nodes inside each cell is shown to be $O(\log |\vec{D}^{(l)}|)$; hence, by deploying a buffer coordination algorithm the end-to-end probability of packet loss is strictly bounded away from 1. With fading, the number of nodes inside each cell together with the quality of the links with their neighboring cells determine whether or not they can communicate with each other.

As stated earlier in Section 5.2, under fading a transmitter picks as the receiver any of the nodes in the neighboring cell whose link with the transmitter has a fading coefficient greater than or equal to g_m. Hence to maintain a constant throughput

inside a streamline region, the coordination algorithm must not only check the availability of free buffer spaces, but also choose nodes such that the fading coefficient requirement is satisfied.

Theorem 5.3 states that adding fading to the Physical Model does not change buffer scalability property of the unit square network.

Theorem 5.3: Adding fading to the Physical Model does not change buffer scalability of the unit square network with $N = O(|\vec{D}^{(l)}|^2 \log |\vec{D}^{(l)}|)$ nodes each having buffer space of size $b = 1$.

Proof. Let l and $(l+1)$ refer to indexes of two adjacent supernodes in the linear network modeling a streamline region. Define the random variable

$$Y_{l,l+1} = \sum_{\substack{k=\{\text{all nodes} \\ \text{in supernode } (l+1)\}}} 1[g_{lk} > g_m],$$

which counts the number of qualified links between the two supernodes for communication. Note that

$$Y_{l,l+1} \sim \text{Binom}(N_{i,j}, P(g_{lk} > g_m))$$

Now based on Lemma 5.3, in order to have a constant throughput in each streamline region, $Y_{l,l+1}$ must be of $O(\log |\vec{D}^{(l)}|)$ for all supernodes along the linear network modeling the region. To show that this event happens w.h.p the following steps must be taken: Let $P = P(g_{lk} > g_m)$, and consider Lemma 5.3; for any desired $\beta > 0$ choose k_1 large enough such that $\frac{\beta}{k_2} < \frac{1}{6}$. Also let $\chi = \frac{\beta \log |\vec{D}^{(l)}|}{N_{i,j}}$. From choices

of k_1 and k_2 it is clear that $\chi < \frac{1}{2}$. Hence,

$$\begin{aligned} P[Y_{l,l+1} \leq \beta \log |\vec{D}^{(l)}|] &= \sum_{\upsilon=0}^{\chi N_{i,j}} \binom{N_{i,j}}{\upsilon} P^{\upsilon}(1-P)^{N_{i,j}-\upsilon} \\ &< 2^{-N_{i,j}} \sum_{\upsilon=0}^{\chi N_{i,j}} \binom{N_{i,j}}{\upsilon} \\ &\leq 2^{-N_{i,j}(1-h(\chi))} \\ &\leq |\vec{D}^{(l)}|^{-\frac{k_2}{3}\log 2(1-h(\chi))} \end{aligned}$$

The assumption $P > \frac{1}{2}$ is used in deriving the first inequality, and the entropy function $h : [0,1] \to [0,1]$ in the second inequality is defined as $h(\chi) = -\chi \log_2 \chi - (1-\chi)\log_2(1-\chi)$. Finally, relation (5.7) is used in deriving the third inequality.

Now using the union bound as $|\vec{D}^{(l)}| \to \infty$,

$$\begin{aligned} P[\bigcap_{l=1}^{\varsigma} \{Y_{l,l+1} > \beta \log |\vec{D}^{(l)}|\}] &\geq 1 - O(|\vec{D}^{(l)}|^{1-\frac{k_2}{3}\log 2(1-h(\chi))}) \\ &\to 1 \qquad \text{if } k_2 > \frac{3}{\log 2(1-h(\chi))} \end{aligned}$$

for which we have substituted $\varsigma = O(|\vec{D}^{(l)}|)$. □

5.4 Summary

In this chapter we investigated the effects of fading on implementability of information flow inside the unit square network. Under a general model of fading, we showed that the previous results (derived in Chapter 4) on sufficient density of nodes to follow flow flux lines need not be changed.

In the second part of this chapter, we investigated buffer scalability of the unit square network. For this purpose, we deviated from using a slotted system and replaced it with an asynchronous system with random service times. By assuming that there is limited or no cross-traffic interference between different streamline regions, each region was modeled as a linear network independently from the rest. Modeling the network as a set of independent linear networks and using the results from linear network analysis, it was shown that with $N = O(|\vec{D}^{(l)}|^2 \log |\vec{D}^{(l)}|)$ nodes deployed uniformly at random inside the square each having buffer space of size $b = 1$, the performance of the unit square network does not degrade as $|\vec{D}^{(l)}| \to \infty$.

Chapter 6

Conclusion and Future Work

6.1 Conclusion

Our focus in this work has been on WSN applications with periodic monitoring requirement, where sensor nodes deployed inside a distributed source send periodic reports to the destination located far away from the source. It is desirable to present a framework to study WSNs that can support more than one application and to provide a means to calculate required density of sensor nodes under different scenarios. To this end, we used a continuous space model called information flow vector field $\vec{D}(x, y)$, with two components (magnitude and direction) at each point in the Euclidean space to model flow of traffic in WSNs.

Information flow flux lines illustrate a set of abstract paths (not constrained by the actual location of sensor nodes) which can be used for data transmission to the destination. During this work, we introduced constraints to place on $\vec{D}$ such that the resulting vector field generates a desirable set of paths.

We also studied the required density of nodes to forward traffic along information flow field. To this end, we divided the network geometry into two parts: within the distributed source, and between the source and destination. Density of sensor nodes inside the distributed source must be such that the whole area is covered and that the active set of nodes constitute a connected set such that all the traffic

generated inside the source can be forwarded to the boundary of this region. On the other hand, nodes outside the distributed source must be connected such that all the traffic generated in the source can be relayed to the destination. Coverage is not an issue for nodes between the distributed source and destination.

We defined a new notion of connectivity (called implementability) which characterizes the ability of sensor nodes to forward traffic along flow flux lines of a given direction field, as the amount of traffic scales linearly to infinity. Using the notion of implementability, we showed that following optimal paths for flow of traffic requires more nodes than providing network connectivity.

The final results indicate that for a given flow field $\vec{D}(x, y)$ which is incompressible and irrotational in the region between the source and destination, a density of $n(x, y) = O(|\vec{D}(x, y)|^2)$ sensor nodes is not sufficient to relay traffic along the flow streamlines. On the other hand, we showed that $\vec{D}(x, y)$ is implementable with a density of $n(x, y) = O(|\vec{D}(x, y)|^2 \log |\vec{D}(x, y)|)$ sensor nodes. We also proposed a joint MAC and routing protocol which requires no more than $n(x, y) = O(|\vec{D}(x, y)|^2 \log |\vec{D}(x, y)|)$ nodes to relay traffic along the flow flux lines. The proposed tier-based scheme also provides a framework to reduce the size of addressing fields (by requiring tier-level addressing instead of node-level addressing) and apply power-saving methods by using clustering techniques, and hence meeting the specific requirements of dense sensor networks. The details of addressing and clustering techniques should be specified based on network geometry and are out of the scope of this work.

We also investigated buffer scalability of sensor nodes forwarding traffic along

flux lines of a given information flow field, and showed that nodes distributed according to the sufficient bound provided above can relay traffic from the source to the destination with each node having a limited buffer space. Furthermore, the results hold in the presence of fading.

6.2 Future Work

This work presented a general framework to study flow of traffic in dense WSNs. Some research topics which are interesting to investigate as future work that were not considered here are as follows.

- Studying the tightness of the sufficiency bound on density of sensor nodes and extending the results for non-ideal flow fields: In Chapters 3 and 4, the sufficient bound on density of sensor nodes was determined by proposing a joint MAC and routing protocol which requires no more than $n(x,y) = O(|\vec{D}(x,y)|^2 \log |\vec{D}(x,y)|)$ nodes to relay traffic along the flow flux lines of a given irrotational flow field $\vec{D}$. However, the tightness of the sufficiency bound was not studied in this work and is left as future work. Also, extending the results of the implementability analysis to non-ideal flow fields (flow vector fields that are solutions of the *p-norm* flow problem with $p \neq 2$) is left as an open problem.

- Performing clustering and tiering techniques in a distributed way: As discussed throughout the work, the proposed tier-based scheme for routing along flow streamlines also provides a framework to reduce the size of addressing fields (by requiring tier-level addressing instead of node-level addressing) and apply power-

saving methods by using clustering techniques. This work can be extended to include distributed addressing and clustering techniques based on network geometry.

- Devising a buffer coordination algorithm: Since sensor nodes have finite buffer space, a buffer coordination algorithm as defined in [8] must be deployed in order to avoid unnecessary network performance degradation. The goal of such algorithm is the efficient use of buffer space in each cell. A buffer coordination algorithm assists nodes in neighboring cells to forward packets to nodes that have available buffer space, when possible. The design of a buffer coordination algorithm was beyond the scope of this dissertation, and we assumed that it could be designed using a token-based approach under the FCFS scheduling policy. The design of such algorithm while considering the limited energy resources of sensor nodes and the necessity of clustering in WSNs is an interesting topic of research.

- Reducing the overhead of periodic reporting: In this work we considered a class of applications which requires continuous monitoring and periodic reporting to the destination. In such applications, it may happen that sensor nodes have very similar readings during long periods of time; hence, it would not be energy efficient for sensors to continuously send the same value to the sink node [66]. It would be interesting to modify the load density function to incorporate a model for rate of change in the sensed data such that data is forwarded to the sink only if it differs from the last transmitted data. This can be seen as a bridge between continuous monitoring and event-driven reporting approaches. Some interesting results are presented in [66] in this regard.

Appendix A

Overview of Fading Channels

The following is a brief discussion on fading channels which is mainly extracted from [41].

Fading is a stochastic variation in the received signal power that may be caused by multipath propagation, scattering, or obstruction [42].

If a single pulse is transmitted over a multipath channel then the received signal will appear as a pulse train, with each pulse in the train corresponding to the Line-of-Sight (LOS) component or a distinct multipath component associated with a distinct scatterer or cluster of scatterers. The time delay spread of a multipath channel can result in significant distortion of the received signal. This delay spread equals the time delay between the arrival of the first received component and the last received signal component associated with a single transmitted pulse.

The impact of multipath on the received signal depends on whether the spread of time delays associated with LOS and different multipath components is large or small relative to the inverse signal bandwidth. If the channel delay spread is small then the LOS and all multipath components are typically non-resolvable, leading to the narrowband fading channel. If the delay spread is large, multipath components are resolvable into some number of discrete components, leading to wideband fading model.

Let the transmitted signal be

$$s(t) = \Re\{u(t)e^{j2\pi f_c t}\},$$

where $u(t)$ is the equivalent lowpass signal for $s(t)$ and f_c is the carrier frequency. The corresponding received signal (ignoring the noise effects) is the sum of the LOS path and all resolvable multipath components:

$$r(t) = \Re\{\sum_{n=0}^{N(t)} \alpha_n(t)u(t-\tau_n(t))e^{j(2\pi f_c(t-\tau_n(t))+\phi_{D_n})}\}, \tag{A.1}$$

where $N(t)$ refers to the number of resolvable multipath components. For each multipath component n, $r_n(t)$ refers to the path length from the transmitter to the receiver, and $\tau_n(t) = \frac{r_n(t)}{c}$ is the corresponding delay[1]. $\phi_{D_n(t)}$ is the Doppler phase shift, and $\alpha_n(t)$ refers to the amplitude. Considering a static network with immobile nodes, the Doppler effect does not play a role.

For typical carrier frequencies f_c, $f_c\tau_n(t) \gg 1$. Hence, a small change in path delay can lead to a large phase change in the nth multipath component. Rapid phase changes in each multipath component give rise to constructive and deconstructive addition of multipath components constituting the received signal, which in turn causes rapid variation in the received signal strength. This phenomenon is called fading.

Suppose the delay spread $T_m \ll B^{-1}$, where B is the bandwidth of the trans-

[1]Here, c refers to the speed of light in vacuum.

mitted signal[2]. Most often, this implies that the delay associated with the ith multipath component $\tau_i \leq T_m$, for all i; hence, $u(t-\tau_i) \approx u(t)$ for all i and (A.1) can be rewritten as

$$r(t) = \Re\Big\{u(t)e^{j2\pi f_c t}\Big(\sum_n \alpha_n(t)e^{-j2\pi f_c \tau_n(t)}\Big)\Big\}$$

For narrowband signals, the received signal can be approximated by

$$r(t) = r_I(t)\cos(2\pi f_c t) - r_Q(t)\sin(2\pi f_c t), \tag{A.2}$$

with the in-phase and quadrature components given by

$$\begin{aligned} r_I(t) &= \sum_{n=1}^{N(t)} \alpha_n(t)\cos(\phi_n(t)), \\ \text{and } r_Q(t) &= \sum_{n=1}^{N(t)} \alpha_n(t)\sin(\phi_n(t)), \end{aligned}$$

where the phase term $\phi_n(t) = 2\pi f_c \tau_n(t) - \phi_0$, with ϕ_0 denoting a random phase offset of the transmitted signal.

Now, based on different assumptions on the existence of a LOS component and position of scatterers, different distributions are suggested for the signal envelope $z(t) = |r(t)| = \sqrt{r_I^2(t) + r_Q^2(t)}$. Nakagami, Ricean, and Rayleigh fading (which is a special case of Nakagami fading) are among some of the distributions commonly used in the literature.

[2]The delay spread T_m for time-varying channels is usually characterized by the rms delay spread, however, it can also be characterized in other ways.

Coherence bandwidth is a statistical measure of the range of frequencies over which the channel has approximately equal gain and linear phase. In other words, coherence bandwidth is the range of frequencies over which any two frequency components have a strong correlation. Channel coherence bandwidth is roughly proportional to $\frac{1}{\text{maximum delay spread}}$.

In general, if we are transmitting a narrowband signal with bandwidth $B \ll B_c$, then fading across the entire signal bandwidth is highly correlated; that is, the fading is roughly equal across the entire signal bandwidth. This is usually referred to as flat fading. On the other hand, if the signal bandwidth $B \gg B_c$, then the channel amplitude values at frequencies separated by more than the coherence bandwidth are roughly independent. Thus, the channel amplitude varies widely across the signal bandwidth. In this case the fading is called frequency selective.

Also it is important to note that fading is a spatial phenomenon, i.e., the fading level depends on the position of a node and only varies over time if the transmitting and/or receiving nodes (or objects in their surroundings) move [42]. To make this distinction, the terms static and dynamic fading are used in the literature. In static fading, only one channel realization is observed over time, whereas a dynamic fading process is usually ergodic. Static fading occurs in networks with static nodes that are placed in rich-scattering environments. A prominent example of static fading occurs in sensor networks [42].

Appendix B

Scheduling Schemes (Proof of Theorem 4.3)

B.1 Scheduling Based on the Protocol Model:

First we need to choose M and the transmission radius r_t such that communication between nodes inside each streamline region is feasible under the Protocol Model without producing significant amount of interference for the rest of the network.

- Choosing a suitable M: For communication to occur between sensor nodes in different cells, a node must at least be able to communicate with nodes in its adjacent cells. Therefore, the transmission radius $r_t \geq 2\sqrt{2}s$.

  For N nodes $X_1^{(l)}, \cdots, X_N^{(l)}$ uniformly distributed inside the unit square, node $X_i^{(l)} \in GC_m$ communicates successfully to node $X_j^{(l)}$ if ,

$$|X_i^{(l)} - X_j^{(l)}| \leq r_t$$

$$\text{and} \quad |X_k^{(l)} - X_j^{(l)}| \geq (1+\Delta)r_t, \quad \forall X_k^{(l)} \in GC_m.$$

  With the aforementioned square tessellation, $\min_{X_k^{(l)} \in GC_m} |X_k^{(l)} - X_j^{(l)}| = (M-2)s$; hence, in order to meet the second constraint of the Protocol Model,

$$(M-2)s \geq (1+\Delta)r_t \tag{B.1}$$

Now choosing $r_t = 2\sqrt{2}s$, and substituting it in (B.1) results in the following lower bound on M:

$$M \geq 2\sqrt{2}(1+\Delta) + 2 = M_{pro} \tag{B.2}$$

Therefore M must be greater than or equal to M_{pro} to communicate based on the Protocol Model inside the unit square using a TDMA scheme with M^2 slots per time frame.

In order to ensure that the traffic of each implementation strip stays within itself the wireless channel is divided into $\kappa \geq 2$ sub-channels of equal capacity $\{C_i = \frac{C}{\kappa}, i = 1, \cdots, \kappa\}$. Let $\kappa = 2$ for the rest of the analysis, and assume that every other streamline region shares the same channel.

- Choosing the transmission radius function: Let r_t denote the transmission radius of each node. Based on the Protocol Model, in order to avoid significant interference between nodes in two different strips sharing the same channel, the distance between every other strip, which is equal to W_s, must satisfy

$$W_s \geq r_t(1+\Delta) \tag{B.3}$$

This relation suggests that, when using two sub-channels, the transmission radius can be chosen to be $r_t = \frac{W_s}{1+\Delta}$; choosing the maximum radius possible is consistent with the overall goal of minimizing the total number of nodes required to follow flow streamlines. In a similar analysis, the transmission

radius in a general case of having $\kappa \geq 2$ sub-channels is equal to $r_t = \frac{(\kappa-1)W_s}{1+\Delta}$, which is linearly proportional to $W_s = O(|\vec{D}^{(l)}|^{-1})$.

Finally, in order to show that a total number of $N = O(|\vec{D}^{(l)}|^2 \log |\vec{D}^{(l)}|)$ nodes is sufficient to follow flow streamlines using the prescribed scheduling scheme, we need to show that there exists at least one node inside each square cell of size s to relay information to its neighboring cells. Let $N_{a,b}$ denote the number of nodes inside cell $C_{a,b}$ and define $\Upsilon_{a,b}$ as the event $\{N_{a,b} > 0\}$. Now, $P[\bigcap_{a,b=1}^{\frac{1}{s}} \Upsilon_{a,b}]$ is the probability of the event that there exists at least one node inside each cell that can be lower bounded as follows:

$$\begin{aligned} P[\bigcap_{a,b=1}^{\frac{1}{s}} \Upsilon_{a,b}] &= 1 - P[\bigcup_{a,b=1}^{\frac{1}{s}} \Upsilon_{a,b}^c] \\ &\geq 1 - \sum_{a,b=1}^{\frac{1}{s}} P[\Upsilon_{a,b}^c] \\ &= 1 - \frac{1}{s^2}(1-s^2)^N \\ &\geq 1 - \exp\Big(- (\log s^2 + Ns^2)\Big) \end{aligned}$$

$\Upsilon_{a,b}^c$ is the complement of $\Upsilon_{a,b}$ and is the event $\{N_{a,b} = 0\}$. Lemma 2 is used in deriving the last inequality. By substituting $N = k|\vec{D}^{(l)}|^2 \log |\vec{D}^{(l)}|$, $n_s(U_2) = \frac{|\vec{D}^{(l)}|}{\gamma C}$ and $s = \frac{r_t}{2\sqrt{2}} = \frac{\gamma C}{2\sqrt{2}(1+\Delta)}|\vec{D}^{(l)}|^{-1}$, and taking the limit as $|\vec{D}^{(l)}| \to \infty$,

$$\begin{aligned} \lim_{|\vec{D}^{(l)}|\to\infty} P[\bigcap_{a,b=1}^{\frac{1}{s}} \Upsilon_{a,b}] \geq 1 - \\ \lim_{|\vec{D}^{(l)}|\to\infty} \frac{8(1+\Delta)^2}{\gamma^2 C^2} \exp\Big(- (k\frac{\gamma^2 C^2}{8(1+\Delta)^2} - 2)\log |\vec{D}^{(l)}|\Big) \end{aligned} \tag{B.4}$$

Therefore if we choose $k > \frac{16(1+\Delta)^2}{\gamma^2 C^2}$, the exponential term in (B.4) goes to zero, and there exists at least one node inside each square cell with probability one as $|\vec{D}^{(l)}| \to \infty$.

Below is a summary of the scheduling scheme presented in this section for relaying traffic along flow streamlines within the unit square based on the Protocol Model:

- Choose $M \geq M_{pro}$
- Set $r_t = \frac{(\kappa-1)W_s}{1+\Delta}$
- Tessellate the unit square into square cells of size $s = \frac{r_t}{2\sqrt{2}}$: $\{C_{a,b}, a, b = 1, \cdots, \frac{1}{s}\}$
- Divide cells into M^2 groups $\{GC_i, i = 1, \cdots, M^2\}$ such that two cells $C_{a,b}$ and $C_{a',b'}$ are in the same group if and only if $a \equiv a' \pmod{M}$, and $b \equiv b' \pmod{M}$
- At each time slot m, nodes inside GC_m send their traffic to their neighboring cell. For this, we assume that each cell has a representative (cluster head) which relays information to the neighboring cell within the same strip and with the most progress toward the bottom of the square.
- Nodes in adjacent strips use different sub-channels to communicate. Therefore, traffic cannot cross and is conserved within the boundaries of strips.

B.2 Scheduling Based on the Physical Model

As mentioned earlier, in a homogeneous scenario, a communication between two nodes $X_i^{(l)}$ and $X_j^{(l)}$ is successful under the Physical Model if

$$\frac{\frac{p_t}{|X_i^{(l)}-X_j^{(l)}|^\alpha}}{N_0+\sum_{\substack{k\in T\\ k\neq i}}\frac{p_t}{|X_k^{(l)}-X_j^{(l)}|^\alpha}}\geq\Gamma, \tag{B.5}$$

where $\{X_k^{(l)}, k\in T\}$ is the set of nodes simultaneously transmitting over the same sub-channel. Due to symmetry in the problem and uniformity of flow field, nodes within the unit square are assumed to have similar transmission power p_t.

The same scheduling scheme proposed for the Protocol Model can be used for the Physical Model to show the sufficiency of $N=O(|\vec{D}^{(l)}|^2\log|\vec{D}^{(l)}|)$ nodes to follow the flow streamlines . Therefore, once again the unit square is tessellated into square cells of size $s=O(|\vec{D}^{(l)}|^{-1})$, and cells are divided into M^2 groups for a fixed positive integer M, similar to the Protocol Model. As the width of streamline regions decreases proportional to $|\vec{D}^{(l)}|^{-1}$, the distance between nodes in adjacent cells responsible for transmission and reception of traffic also decreases with the same proportion. Therefore, to reduce the energy consumption of nodes and limit the amount of interference to neighboring regions, transmission power p_t must scale proportional to $|\vec{D}^{(l)}|^{-\alpha}$. Now the same TDMA scheme can be used for nodes to relay traffic to their neighboring cells. The only question left is to specify how to choose M such that communication between nodes in different cells are successful under the Physical Model. For this, we have to find a finite M independent of θ

Table B.1: Minimum distance between $X_j^{(l)}$ and nodes simultaneously active with $X_i^{(l)}$

tier	number of active cells	$\min \lvert X_k^{(l)} - X_j^{(l)} \rvert$
1	8	$(M-2)s$
2	16	$(2M-2)s$
$\vdots$	$\vdots$	$\vdots$
v	$8v$	$(vM-2)s$

such that the SINR bound can be met. This can be done by imposing the threshold constraint on a lower bound of the SINR ratio.

Let p_r denote the received power at a node. Since nodes communicate only with their neighboring cells,

$$p_r \geq \frac{p_t}{(2\sqrt{2}s)^\alpha} \tag{B.6}$$

On the other hand, the total interference generated by simultaneous transmissions from nodes in the same group can be upper bounded as described below. Let $X_i^{(l)}$ be a node inside the dashed cell in the center of the square shown in Fig. B.1, and let $\{X_k^{(l)}, k \in T\}$ denote all nodes transmitting in the same time slot and sub-channel as $X_i^{(l)}$. Cells that are simultaneously active with the central cell when $M = 2$ are shaded in Fig. B.1. These cells occupy different tiers, and can be categorized as described in Table B.1.

Based on Table B.1, the total interference $I(M)$ which is a function of M can

be upper bounded as follows:

$$\begin{aligned} I(M) &\leq \sum_{v=1}^{\infty} 8v \frac{p_t}{\big((vM-2)s\big)^{\alpha}} \\ &= \frac{8p_t}{Ms^{\alpha}} \sum_{v=1}^{\infty} \frac{vM-2+2}{(vM-2)^{\alpha}} \\ &= \frac{8p_t}{Ms^{\alpha}} [\sum_{v=1}^{\infty} \frac{1}{(vM-2)^{\alpha-1}} + 2\sum_{v=1}^{\infty} \frac{1}{(vM-2)^{\alpha}}] \\ &\leq \frac{8p_t}{Ms^{\alpha}} [\sum_{v=1}^{\infty} v^{-\alpha+1} + 2\sum_{v=1}^{\infty} v^{-\alpha}] \\ &= \frac{8p_t}{Ms^{\alpha}} [\zeta(\alpha-1) + 2\zeta(\alpha)] \end{aligned} \tag{B.7}$$

Both series in the fourth line of relation (B.7) converge if $\alpha > 2$. In the last equality, we have defined function $\zeta : \mathbb{R} \to \mathbb{R}^{+}$, and have substituted $\zeta(\alpha) = \sum_{v=1}^{\infty} v^{-\alpha}$ to emphasize that the convergent series is only a function of α.

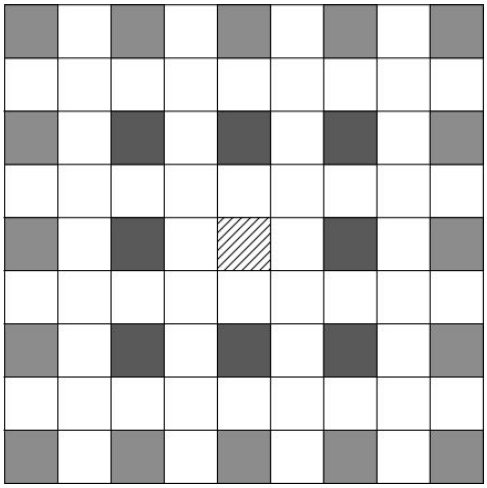

Figure B.1: Cells simultaneously active with the central cell when $M = 2$.

Based on relations (B.6) and (B.7), the total SINR ratio can be lower bounded

by

$$SINR \geq \frac{\frac{p_t}{(2\sqrt{2})^\alpha}}{N_0 s^\alpha + \frac{8p_t}{M}[f(\alpha-1)+2f(\alpha)]} \tag{B.8}$$

Now, in order to find a suitable range for M such that simultaneous transmissions are successful based on the Physical Model,

$$\begin{aligned} &\frac{\frac{p_t}{(2\sqrt{2})^\alpha}}{N_0 s^\alpha + \frac{8p_t}{M}[f(\alpha-1)+2f(\alpha)]} \geq \Gamma \\ \text{therefore,} \quad &M \geq \frac{8[f(\alpha-1)+2f(\alpha)]}{\frac{1}{\Gamma(2\sqrt{2})^\alpha} - N_0\frac{s^\alpha}{p_t}} = M_{phy} \end{aligned} \tag{B.9}$$

Note that since $s = O(|\vec{D}^{(l)}|^{-1})$ and $p_t = O(|\vec{D}^{(l)}|^{-\alpha})$, the second term in the denominator of M_{phy}, $N_0\frac{s^\alpha}{p_t}$, converges to a constant number as $|\vec{D}^{(l)}| \to \infty$. Furthermore, p_t can be chosen such that the denominator is positive. Therefore, M_{phy} is a fixed number and the SINR does not grow as the total number of nodes grows to infinity.

Hence, provided $M \geq M_{phy}$, the same TDMA scheme with M^2 slots per time frame can be used to carry traffic within streamline regions of the unit square.

Bibliography

[1] M. Kalantari and M. Shayman. Energy efficient routing in wireless sensor networks. In *Proceedings of Conference on Information Sciences and Systems*, 2004.

[2] M. Kalantari and M. Shayman. Routing in wireless ad hoc networks by analogy to electrostatic theory. In *2004 IEEE International Conference on Communications*, vol. 7, 2004.

[3] M. Kalantari and M. Shayman. Routing in multi-commodity sensor networks based on partial differential equations. In *40th Annual Conference on Information Sciences and Systems*, pp. 402–406, 2006.

[4] M. Kalantari, M. Haghpanahi, and M. Shayman. A p-norm flow optimization problem in dense wireless sensor networks. In *IEEE INFOCOM 2008. The 27th Conference on Computer Communications*, pp. 341–345, 2008.

[5] S. Kulkarni, A. Iyer, and C. Rosenberg. An address-light, integrated MAC and routing protocol for wireless sensor networks. *IEEE/ACM Transactions on Networking*, vol. 14, no. 4, pp. 793–806, 2006.

[6] C. Shanti and A. Sahoo. DGRAM: a delay guaranteed routing and MAC protocol for wireless sensor networks. *IEEE Transactions on Mobile Computing*, pp. 1407–1423, 2010.

[7] S. Toumpis and A. Goldsmith. Large wireless networks under fading, mobility, and delay constraints. In *IEEE INFOCOM 2004*, pp. 609–619, 2004.

[8] P. R. Jelenković, P. Momčilović, and M. S. Squillante. Scalability of wireless networks. *IEEE/ACM Transactions on Networking*, vol. 15, no. 2, pp. 295–308, 2007.

[9] P. Momčilović and M. S. Squillante. On throughput in linear wireless networks. In *Proceedings of the 9th ACM International Symposium on Mobile Ad Hoc Networking and Computing*, pp. 199–208, Hong Kong, China, 2008.

[10] S. Toumpis, L. Tassiulas. Packetostatics: deployment of massively dense sensor networks as an electrostatics problem. In *Proceedings of IEEE INFOCOM 2005. 24th Annual Joint Conference of the IEEE Computer and Communications Societies*, vol. 4, 2005.

[11] J. N. Al-Karaki and A. E. Kamal. Routing techniques in wireless sensor networks: a survey. *IEEE Wireless Communications*, vol. 11, no. 6, pp. 6–28, 2004.

[12] P. Gupta and P. R. Kumar. Critical power for asymptotic connectivity. In *Proceedings of the 37th IEEE Conference on Decision and Control*, vol. 1, pp. 1106–1110, 1998.

[13] P. Gupta and P. R. Kumar. The capacity of wireless networks. *IEEE Transactions on Information Theory*, vol. 46, no. 2, pp. 388–404, 2000.

[14] S. Kulkarni, A. Iyer, C. Rosenberg, and D. Kofman. Routing dependent node density requirements for connectivity in multi-hop wireless networks. In *IEEE GLOBECOM '04*, vol. 5, pp. 2890–2896, 2004.

[15] N. T. Nguyen, A. I. A. Wang, P. Reiher, and G. Kuenning. Electric-field-based routing: a reliable framework for routing in MANETs. *ACM SIGMOBILE Mobile Computing and Communications Review*, vol. 8, no. 2, pp. 35–49, 2004.

[16] V. Lenders and R. Baumann. Link-diversity routing: a robust routing paradigm for mobile ad hoc networks. In *IEEE Wireless Communications and Networking Conference*, pp. 2585–2590, 2008.

[17] N. Kemmer. *Vector Analysis: A Physicist's Guide to the Mathematics of Fields in Three Dimensions*. Cambridge University Press, 1977.

[18] P. Knupp. Mesh generation using vector-fields. *Journal of Computational Physics*, vol. 119, no. 1, pp. 142–148, 1995.

[19] M. Kalantari and M. Shayman. Design optimization of multi-sink sensor networks by analogy to electrostatic theory. In *IEEE Wireless Communications and Networking Conference*. , 2006.

[20] M. Kalantari. *Design optimization and security for communication networks*. PhD thesis, University of Maryland, College Park, 2005.

[21] S. Verma and K. Aziz. A control volume scheme for flexible grids in reservoir simulation. In *SPE Reservoir Simulation Symposium*, 1997.

[22] M. Edwards, R. Elf, and K. Aziz. Quasi K-orthogonal streamline grids: gridding and discretization. In *SPE Annual Technical Conference and Exhibition*, 1998.

[23] A. Castellini, M.G. Edwards, and L.J. Durlofsky. Flow based modules for grid generation in two and three dimensions. In *Proceedings of the 7th European Conference on the Mathematics of Oil Recovery, Baveno, Italy*, 2000.

[24] P. Santi. *Topology Control in Wireless Ad Hoc and Sensor Networks*. Wiley, 2005.

[25] M. Franceschetti, O. Dousse, D. N. C. Tse, and P. Thiran. Closing the gap in the capacity of wireless networks via percolation theory. *IEEE Transactions on Information Theory*, vol. 53, no. 3, pp. 1009–1018, 2007.

[26] P. J. Olver. *Applied Mathematics Lecture Notes*. http://www.math.umn.edu/ olver/appl.html

[27] D. K. Cheng. *Field and Wave Electromagnetics*. Addison-Wesley, 1989.

[28] D. M. Blough, C. Canali, G. Resta, and P. Santi. On the impact of far-away interference on evaluations of wireless multihop networks. In *Proceedings of the 12th ACM International Conference on Modeling, Analysis and Simulation of Wireless and Mobile Systems*, pp. 90–95, 2009.

[29] A. Basu, A. Lin, and S. Ramanathan. Routing using potentials: a dynamic traffic-aware routing algorithm. In *Proceedings of the 2003 Conference on Applications, Technologies, Architectures, and Protocols for Computer Communications*, pp. 37–48, Karlsruhe, Germany, 2003.

[30] P. Knupp and S. Steinberg. *Fundamentals of Grid Generation*. CRC Press, 1993.

[31] K. Akkaya and M. Younis. A survey on routing protocols for wireless sensor networks. *Ad Hoc Network Journal*, vol. 3, no. 3, pp. 325–349, 2005.

[32] W. B. Heinzelman, A. P. Chandrakasan, and H. Balakrishnan. An application-specific protocol architecture for wireless microsensor networks. *IEEE Transactions on Wireless Communications*, vol. 1, no. 4, pp. 660–670, 2002.

[33] H. Zhang and J. C. Hou. Maintaining sensing coverage and connectivity in large sensor networks. *Ad Hoc & Sensor Wireless Networks*, vol. 14, no. 28, 2005.

[34] X. Wang, G. Xing, Y. Zhang, C. Lu, R. Pless, and C. Gill. Integrated coverage and connectivity configuration in wireless sensor networks. In *Proceedings of the 1st ACM International Conference on Embedded Networked Sensor Systems*, pp. 28–39, 2003.

[35] T. Shu, M. Krunz, and S. Vrudhula. Power balanced coverage-time optimization for clustered wireless sensor networks. In *Proceedings of the 6th ACM International Symposium on Mobile Ad Hoc Networking and Computing*, pp. 111–120, 2005.

[36] O. Younis, M. Krunz, and S. Ramasubramanian. Node clustering in wireless sensor networks: recent developments and deployment challenges. *IEEE Network*, vol. 20, no. 3, pp. 20–25, 2006.

[37] A. Ghosh and S. K. Das. Coverage and connectivity issues in wireless sensor networks: A survey. *Pervasive and Mobile Computing*, vol. 4, no. 3, pp. 303–334, 2008.

[38] P. Cardieri. Modeling interference in wireless ad hoc networks. *Communications Surveys & Tutorials, IEEE*, vol. 12, no. 4, pp. 551–572, 2010.

[39] G. Barrenetxea, B. Berefull-Lozano, and M. Vetterli. Lattice networks: capacity limits, optimal routing, and queueing behavior. *IEEE/ACM Transactions on Networking*, vol. 14, no. 3, pp. 492–505, 2006.

[40] S. Toumpis and L. Tassiulas. Optimal deployment of large wireless sensor networks. *IEEE Transactions on Information Theory*, vol. 52, no. 7, pp. 2935–2953, 2006.

[41] A. Goldsmith. *Wireless Communications*. Cambridge University Press, 2005.

[42] M. Haenggi. Link modeling with joint fading and distance uncertainty. *4th IEEE International Symposium on Modeling and Optimization in Mobile, Ad Hoc and Wireless Networks*, 2006.

[43] R. K. Ahuja, T. L. Magnanti, and J. B. Orlin. *Network Flows: Theory, Algorithms, and Applications*. Prentice-Hall, Englewood Cliffs, NJ, 1993.

[44] D. Guo and S. Verdu. Replica analysis of large-system CDMA. In *Proceedings of IEEE Information Theory Workshop*, 2003.

[45] A. El Gamal, J. Mammen, B. Prabhakar, and D. Shah. Throughput-delay trade-off in wireless networks. In *Proceedings of IEEE INFOCOM*, 2004.

[46] M. Alicherry, R. Bhatia, and L. E. Li. Joint channel assignment and routing for throughput optimization in multi-radio wireless mesh networks. In *Proceedings of the 11th Annual International Conference on Mobile Computing and Networking*, pp. 58–72, Cologne, Germany, 2005.

[47] R. Durrett. *Probability: Theory and Examples*. Cambridge University Press, 2010.

[48] T. Liu and W. Liao. Location-dependent throughput and delay in wireless mesh networks. *IEEE Transactions on Vehicular Technology*, vol. 57, no. 2, pp. 1188–1198, 2008.

[49] A. Al-Hanbali, A. A. Kherani, R. Groenevelt, P. Nain, and E. Altman. Impact of mobility on the performance of relaying in ad hoc networks. In *Proceedings of IEEE INFOCOM 2006 Conference*, 2006.

[50] K. Akkaya and M. Younis. An energy-aware QoS routing protocol for wireless sensor networks. In *Proceedings of 23rd International Conference on Distributed Computing Systems Workshops*, pp. 710–715, Rhode Island, USA, 2003.

[51] N. Bisnik and A. Abouzeid. Delay and throughput in random access wireless mesh networks. In *2006 IEEE International Conference on Communications*, pp. 403–408, Istanbul, 2006.

[52] D. P. Bertsekas and R. G. Gallager. *Data Networks*. Englewood Cliffs, NJ: Prentice-Hall, 1992.

[53] R. Motwani and P. Raghavan. *Randomized Algorithms*. Cambridge University Press, 1995.

[54] S. Toumpis. Mother nature knows best: a survey of recent results on wireless networks based on analogies with physics. *Computer Networks*, vol. 52, no. 2, pp. 360–383, 2008.

[55] E. A. Varvarigos and D. P. Bertsekas. Performance of hypercube routing schemes with or without buffering. *IEEE/ACM Transactions on Networking*, vol. 2, no. 3, pp. 299–311, 1994.

[56] S. Toumpis. *Capacity and cross-layer design of wireless ad hoc networks*. PhD thesis, Stanford university, 2003.

[57] P. Jacquet. Geometry of information propagation in massively dense ad hoc networks. In *Proceedings of the 5th ACM International Symposium on Mobile Ad Hoc Networking and Computing*, pp. 157–162, Tokyo, Japan, 2004.

[58] R. Catanuto, G. Morabito, and S. Toumpis. Optical routing in massively dense networks: practical issues and dynamic programming interpretation. In *Proceedings of International Symposium on Wireless Communications Systems*.

[59] R. Catanuto, S. Toumpis, and G. Morabito. Opti{c, m}al: optical/optimal routing in massively dense wireless networks. In *Proceedings of IEEE INFOCOM*, pp. 1010–1018, 2007.

[60] A. Cerpa, J. Elson, D. Estrin, L. Girod, M. Hamilton, and J. Zhao. Habitat monitoring: application driver for wireless communications technology. *ACM SIGCOMM Computer Communication Review*, vol. 31, no. 2 supplement, pp. 20–41, 2001.

[61] J. Hill, R. Szewczyk, A. Woo, S. Hollar, D. Culler, and K. Pister. System architecture directions for networked sensors. *ACM Sigplan Notices*, vol. 35, no. 11, pp. 93–104, 2000.

[62] J. M. Kahn, R. H. Katz, and K. S. J. Pister. Next century challenges: mobile networking for "smart dust". In *Proceedings of the 5th Annual ACM/IEEE International Conference on Mobile Computing and Networking*, pp. 271–278, NY, USA, 1999.

[63] G. J. Pottie and W. J. Kaiser. Wireless integrated network sensors. *Communications of the ACM*, vol. 43, no. 5, pp. 51–58, 2000.

[64] J. Warrior. Smart sensor networks of the future. *Sensors Magazine*, vol. 14, no. 3, pp. 40–45, 1997.

[65] K. A. Ross. *Elementary Analysis: The Theory of Calculus*. Springer Verlag, 1980.

[66] N. Bouabdallah, M. E. Rivero-Angeles, and B. Sericola Continuous monitoring using event-driven reporting for cluster-based wireless sensor networks. *IEEE Transactions on Vehicular Technology*, vol. 58, no. 7, pp. 3460–3479, 2009.

[67] http://www.isi.edu/nsnam/ns2/

[68] G. F. Riley. The Georgia Tech network simulator. In *Proceedings of the ACM SIGCOMM Workshop on Models, Methods and Tools for Reproducible Network Research*, pp. 5–12, 2003.